npj | heritage science

Article

https://doi.org/10.1038/s40494-025-02116-9

Chemical evidence for the spread of lac colorant in Xinjiang from the 2nd to 9th centuries CE

Check for updates

Sihan Zhao[1,11], Juan Zhang[1,11], Ana Serrano[2], Diego Tamburini[3], Xiaojing Kang[4], Zhibo Zhou[5], Yumin Gao[6], Ling Shen[7], Jiakun Wang[1], Jie Yang[5], Shaowen Shi[8], Jian Liu[9,10] ✉ & Hui Zhang[1] ✉

Lac dye, indigenous to South and Southeast Asia, is historically accepted to have entered Xinjiang during the Han Dynasty through trade routes established between India and China, and later from the 5th century CE, when Buddhist art started flourishing in the region. The dynamics of trade and colorant applications of lac in the region has been constrained by the limited availability of historical written sources, archeological materials, and scientific investigations. Using ultra-performance liquid chromatography with photo diode array detection and mass spectrometry (UPLC-PDA-MS), this study explores the characterization of lac in a small group of archeological textiles, wall paintings, and painted sculptures, dated between the 2nd and 9th century CE. It aims to undertake a first attempt to historically trace the dissemination of the insect dye between India and Northwest China, and within the broader framework of trade and cultural exchange along the Silk Roads in the first millennium CE.

Insect dyes have been highly regarded since ancient times for providing lasting and bright shades of red color, representing luxury and prestige. These dyes were among the most expensive colorants, and the raw insects were also one of the most profitable trading goods among continents in history. The most common sources of Eurasian insect dyes found in ancient historical literature are scale insects of the superfamily Coccoidea, including lac (*Kerria lacca* Kerr and other *Kerria* and *Paratachardina* species), kermes (*Kermes vermilio* Planchon), Polish cochineal (*Porphyrophora polonica* Linnaeus), and Armenian cochineal (*Porphyrophora hamelii* Brandt). The term "cochineal" specifically refers to Polish and Armenian cochineal in the following text.

Red colorants extracted from these insects are anthraquinone molecules, such as kermesic acid, carminic acid and laccaic acid A, which have been used to dye wool and silk since antiquity, producing colors ranging from purple to orange, depending on dyeing processes and mordants[1]. Kermesic acid and carminic acid colorants only exist within the female scale insect's body, which means that kermes and cochineal insects need to be killed and crushed to extract the red dyes, while lac dye can be extracted from the resin without killing the insects. To isolate the dye from the resin, crude lac was traditionally ground into a fine powder and treated with a dilute base solution, which extracted the coloring matter. This extract was subsequently precipitated by adding an alum solution and then evaporated to produce lac dye[1].

Kermes insects occur in coastal regions around the Mediterranean Sea. Polish and Armenian cochineal (along other *Porphyrophora* species) were widespread throughout the Palearctic region, including North of the Himalayas, and both Central and East Europe, where a characteristic biotope of steppe environment dominates[1]. Polish cochineal appears to have been used as a textile dye by the 1st century BCE by Central European communities, and would only be levied from the middle of the first millennium CE by the Roman-Byzantine authorities[2]. Further east, Armenian historians and geographers wrote in the 5th century BCE that insects grew in the Ararat valley and were sold for dyeing purposes. These insects were very likely Armenian cochineal, which was historically recorded to be found among the booty plundered by the Assyrians around 714 BCE[3]. Lac dye is part of

[1]School of Art and Archaeology, Zhejiang University, Hangzhou, China. [2]University of Amsterdam, Faculty of Humanities, Amsterdam School for Heritage, Memory and Material Culture, Conservation and Restoration of Cultural Heritage, Amsterdam, The Netherlands. [3]Department of Scientific Research, British Museum, Great Russell Street, WC1B 3DG, London, United Kingdom. [4]The Cultural Relics and Archaeology Institute of Xinjiang Uygur Autonomous Region, Urumqi, China. [5]Conservation and Restoration Department, The Kucha Academy of Xinjiang, Urumqi, China. [6]Xinjiang Uygur Autonomous Region Museum, Urumqi, China. [7]Department of Archaeology, Hangzhou City University, Hangzhou, China. [8]ZJU-Hangzhou Global Scientific and Technological Innovation Center, Hangzhou, China. [9]Key Scientific Research Base of the Textile Conservation, National Cultural Heritage Administration, China National Silk Museum, Hangzhou, China. [10]Department of Applied Chemistry, College of Chemical Engineering, Zhejiang University of Technology, Hangzhou, China. [11]These authors contributed equally: Sihan Zhao, Juan Zhang. ✉e-mail: liujian@cnsilkmuseum.org; huizhang@zju.edu.cn

the resinous secretion produced by scale insects of the *Kerria, Paratachardina* and other species, of which the Indian *Kerria Lacca* is the most common one in human culture. This dye has been used in India for more than 4000 years, being appreciated for its excellent dyeing ability since the end of the Vedic period[4].

At the turning to the 1st millennium CE, kermes and cochineal were the main sources of insect dyes in Europe, West Asia and North Africa, as furthermore attested by the identified presence of these dyes in textile fragments found in Roman archeological sites located in Egypt and Syria[5,6]. In contrast, lac-dyed textiles, imported from South and Southeast Asia, appear to have been sparsely available in these regions[7]. In Xinjiang and its surrounding regions, lac, as well as kermes and cochineal, have been reported in a few excavated textiles[8–11], suggesting the travel of these insect materials from West and South Asia into Northwest China from the 3rd century BCE to the 10th century CE.

Xinjiang, located in the hinterland of the vast central Eurasian continent, is a historically significant crossroad of various cultures and trade routes since ancient times. This territory not only bridges the West Asian and the Eastern civilizations, but is also open to the Steppe of the North, and has long-lasting ties with India. Previous archeological studies indicated that as early as the 2nd millennium BCE, the Steppe peoples of the Late Bronze Age and Early Iron Age mingled with the indigenous peoples in Xinjiang[12]. Agricultural plants, animals, technologies, religious beliefs, artefacts and trade subsequently traversed into East Asia through Xinjiang along with the migration and mixing of people at that time[13,14]. With the rise of the Silk Road, Xinjiang played an increasingly important role in the cultural exchanges between East and West. Especially around the 1st century BCE, Buddhism began to spread from India northwards, gradually entering Xinjiang. As an important stop for the spread of Buddhism, Xinjiang witnessed the prosperity and development of Buddhist culture. The Kizil and Simsim Grottoes in the Kucha area are outstanding representatives of Buddhist art in Xinjiang. These caves are not only places of Buddhist practice and worship, they are also surviving treasure repositories of ancient artistry, with their intricate wall paintings, richly-made textiles, and painted sculptures and potteries. The decorative patterns, styles, and dyes found in many of these objects reflect the influence of foreign cultures, such as those of West Asia or the Eurasian Steppe[15–17].

Despite great efforts in describing the spread and exchange of metals, cash crops and pottery in Eurasia, little scientific research has been paid to insect-derived materials with regional characteristics, such as lac. Historical context about trade and colorant applications of lac dye in Xinjiang is usually limited by the scant availability of historical written sources, archeological materials, and scientific investigation. This study attempts to historically trace the dissemination of lac dye in Xinjiang, by combining the geographical location and cultural background of lac, with chemical analysis of surviving archeological objects. Using ultra-performance liquid chromatography with photo diode array detection and mass spectrometry (UPLC-PDA-MS), scanning electron microscope (SEM) and Raman spectroscopy, this study characterizes the presence of lac in fifteen samples taken from archeological textiles, wall paintings, and painted sculptures dated between the 2nd and 9th century CE.

Methods

Objects and samples

Samples were obtained from three archeological textiles from three burial sites in Xinjiang, Miran and Yingpan, located on the southern and eastern rims of the Taklamakan Desert, and Astana, located in the Turpan Basin (Fig. 1). These textiles are extraordinarily well preserved, due largely to the very dry climate of Xinjiang (Fig. 2a, d). An additional silk samite robe lining fragment with horses' roundels of Sogdian origin (MC1) was collected by the China National Silk Museum through intermediaries in Gansu or Qinghai province. In addition, eleven samples of nine wall paintings and painted sculptures (Fig. 2b, c, e–k) were obtained mainly from the Kizil and Simsim Grottoes and Astana Tombs (Fig. 1). The list of samples and associated descriptions are presented in Table 1, and the background of the listed archeological sites is described below:

- Yingpan, Yuli (CE 140 ± 30): The Yingpan Cemetery is located in the Lop Nor area of Xinjiang. In 1995, The Cultural Relics and Archaeology Institute of Xinjiang Uygur Autonomous Region led a team to excavate the cemetery and many textiles (wool, silk, cotton), wooden objects, pottery and ironware were found. The cemetery can be dated back to Eastern Han and Jin Dynasties (CE 25–420). The finding of weaving tools and loom components found in tombs indicate that the recovered woolen textiles could have been produced locally [18].

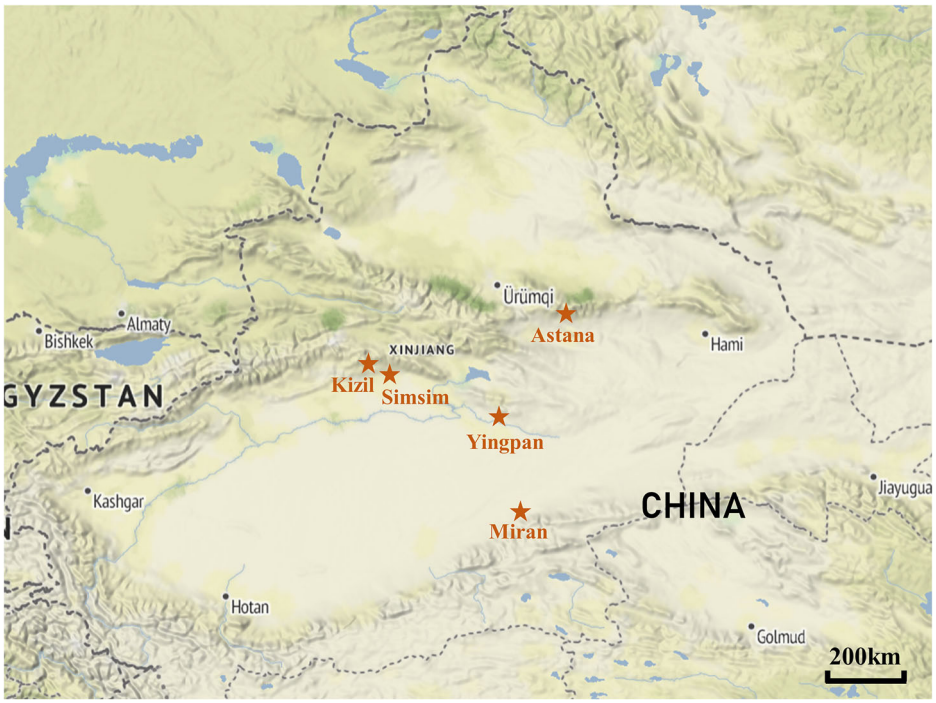

Fig. 1 | Geographic location of the archeological sites studied in this work.

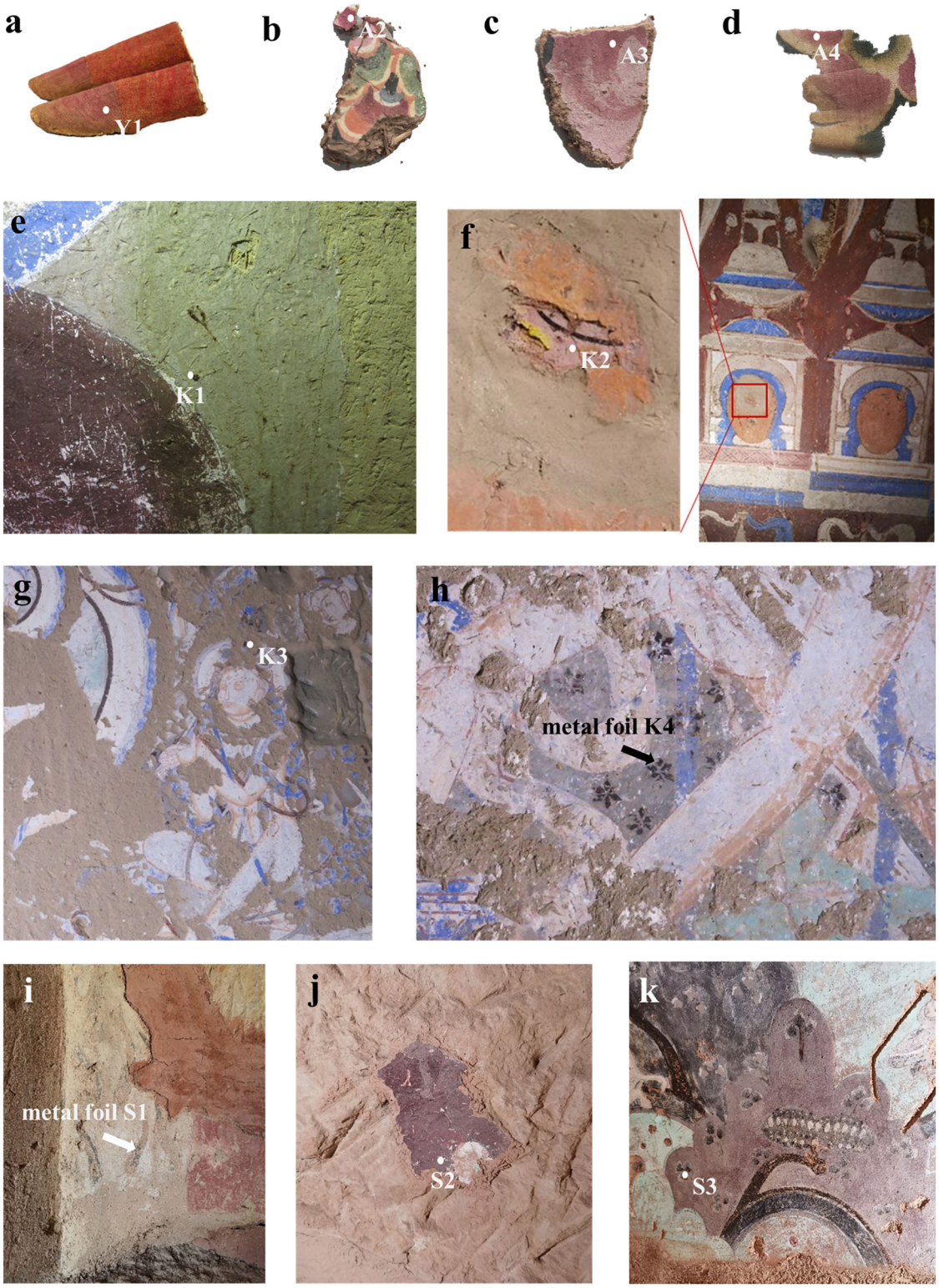

Fig. 2 | Sampling locations of the objects. a Y1 from the Yingpan Cemetery; **b** A2 from 60TAM336, **c** A3 from 72TAM187, and **d** A4 from 73TAM227, from the Astana Tombs; **e** K1, **f** K2, **g** K3, and **h** K4 from Cave 171 in the Kizil Grottoes; and **i** S1 from Cave 1, **j** S2 from Cave 9, and **k** S3 from Cave 14, in the Simsim Grottoes.

- Kizil (CE 5th–7th) and Simsim (CE 5th–9th), Kucha: The Kizil and Simsim Grottoes are two cave complexes located in the north of the Taklamakan desert, in the ancient Kucha area. The Kizil is the earliest major Buddhist cave complex in China, with more than 5000 m^2 wall paintings left. The Simsim is equally covered with colorful wall paintings and architectural cave structures following different styles from Central China, India and even Greece[19,20].
- Astana, Turpan (CE 7th–9th): The Astana Tombs are located near the Turpan basin, and were the public graveyards of the ancient Gaochang people. Thousands of tombs dating from the 3rd to the 9th centuries CE were excavated by the Xinjiang Uyghur Autonomous Region Museum and other institutes during 1959 and 1975. These campaigns recovered from the tombs many painted clay sculptures, pottery, and metallic objects. Due to the extremely dry

Table 1 | List of the archeological textiles and painted objects investigated in this study

Archeological site	Object No.	Description
Yingpan, Yuli (CE 140 ± 30[a])	Y1	Red woolen socks
Kizil, Kucha (CE 5th–7th)	K1 in Cave 171	Red colorant of wall painting
	K2 in Cave 171	Red colorant of wall painting
	K3 in Cave 171	Red colorant of wall painting
	K4 in Cave 171	Gilding adhesive of wall painting
Simsim, Kucha (CE 5th–9th)	S1 in Cave 1	Gilding adhesive of wall painting
	S2 in Cave 9	Red colorant of wall painting
	S3 in Cave 14	Red colorant of wall painting
	S4 in Cave 18	Red colorant of wall painting
Museum collection (CE 6th–9th)	MC1	Robe lining with horses' roundels
Astana, Turpan (CE 7th–9th)	A1 from 72TAM187	Ocher colorant of Painted sculpture
	A2 from 60TAM336	Purplish colorant of Painted sculpture
	A3 from 72TAM187	Dark red colorant of Painted sculpture
	A4 from 73TAM227	Pink yarn
Miran, Charklik (CE 8th–9th)	MR1	Red woolen thread

[a]The textile sample was radiocarbon dated by accelerator mass spectrometry (AMS) at the Beta Analytic Radiocarbon Dating Laboratory.

Table 2 | List of compounds identified in the archeological textiles by UPLC-PDA-MS (negative ion mode)

Samples	Peak no.	Possible compounds	Chemical formula	Calculated mass $[M-H]^-$	Experimental mass $[M-H]^-$
Y1	1	Laccaic acid A	$C_{26}H_{19}NO_{12}$	536.08	536.00
	2	Laccaic acid B	$C_{24}H_{16}O_{12}$	495.06	494.99
	3	Laccaic acid C	$C_{25}H_{17}NO_{13}$	538.06	538.02
	4	Laccaic acid E	$C_{24}H_{17}NO_{11}$	494.07	494.03
A4	1	Laccaic acid A	$C_{26}H_{19}NO_{12}$	536.08	536.05
	2	Laccaic acid B	$C_{24}H_{16}O_{12}$	495.06	494.99
	3	Laccaic acid C	$C_{25}H_{17}NO_{13}$	538.06	538.06
	4	Laccaic acid E	$C_{24}H_{17}NO_{11}$	494.07	494.07
MR1	1	Laccaic acid A	$C_{26}H_{19}NO_{12}$	536.08	536.05
	2	Laccaic acid B	$C_{24}H_{16}O_{12}$	495.06	494.98
	3	Laccaic acid C	$C_{25}H_{17}NO_{13}$	538.06	538.06
	4	Laccaic acid E	$C_{24}H_{17}NO_{11}$	494.07	494.05
MC1	1	Laccaic acid A	$C_{26}H_{19}NO_{12}$	536.08	536.02
	2	Laccaic acid B	$C_{24}H_{16}O_{12}$	495.06	495.06
	3	Laccaic acid C	$C_{25}H_{17}NO_{13}$	538.06	538.06
	4	Laccaic acid E	$C_{24}H_{17}NO_{11}$	494.07	494.05

Calculated masses and experimental masses of the deprotonated molecules $[M-H]^-$ and chemical formulas are reported.

climate in the Turpan basin, many organic remains have been preserved[21].

- Miran, Charklik (CE 8th–9th): The Miran site, located on the Southern edge of the Taklamakan desert, is well known for its "winged angel" wall paintings and diverse cultural artifacts dating from the Han Dynasty to the Tubo Kingdom (~2nd BCE–9th CE). Although the site was excavated in the late 19th century by European archeologists, most remains have been recovered by teams from the Chinese Academy of Social Sciences and the Cultural Relics and Archaeology Institute of Xinjiang Uygur Autonomous Region since 1950[22].

Chemicals and reagents

All solvents were HPLC grade or higher. Methanol and acetonitrile were purchased from Merck (Germany), formic acid and ultra-pure water from Fisher Scientific (USA), and pyridine from ANPEL CNW (China). Oxalic acid (≥98%) was purchased from Acros Organics (USA).

Extraction procedure

Colorants were extracted from about 0.1–0.2 mg of yarn from archeological textiles and about 0.5 mg of sample from painted surfaces by heating in 200 μL of pyridine/water/0.1 M oxalic acid in water (95/95/10) at 80 °C for 30 min. The supernatant solution was transferred to a 1.5 mL centrifuge tube (Eppendorf, Germany), and the extract was evaporated to dryness under a stream of nitrogen, after which the residue was dissolved in 50 μL of MeOH/H_2O (1/1). Subsequently, the solution was centrifuged for 5 min, and 30 μL of supernatant was transferred to a 200 μL microvial (Shimadzu, Japan) for analysis. Then, 20 μL was injected into the UPLC column by an autosampler.

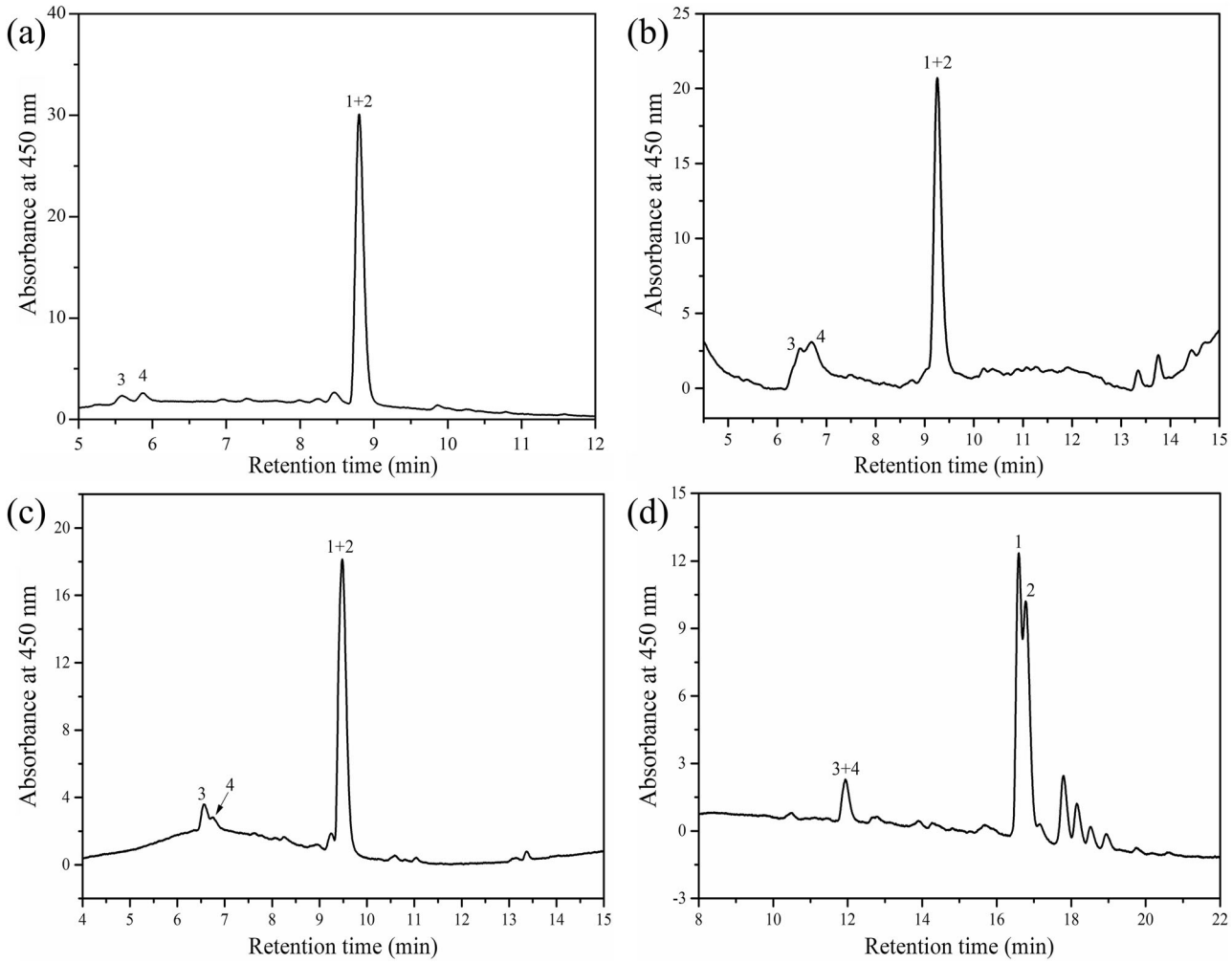

Fig. 3 | HPLC profile of the red dye extracted from the following samples. a Y1, **b** A4, **c** MR1, and **d** MC1. Compounds 1–4 are laccaic acids A, B, C and E, respectively.

Analysis of colorant by UPLC-PDA-MS

Colorant analysis was performed using a UPLC-PDA-MS system consisting of two LC-20AD delivery units, a SPD-M20A photodiode array detector (all Shimadzu, Japan) coupled with an LTQ XL linear ion trap mass spectrometer with an ESI ion source (Thermo, USA). The extract was separated on a Shim-pack XR-ODS column (3.0 mm × 75 mm, 2.2 μm particle size) or a Phenomenex Luna C18 column (2.0 mm × 150 mm, 3.0 μm particle size). The column was eluted with water-acetonitrile gradients containing 0.1% formic acid at a flow rate of 0.3 mL/min[8]. During this research, though several gradient programs were used, the peaks always eluted in the same order, since the types of stationary and mobile phases were not changed.

Multiple-stage mass spectra were obtained and processed by Xcalibur 2.1 software (Thermo, USA) in the mass range of m/z 50-1000. The mass spectrometer parameters were set up as follows: ion spray voltage −2.5 kV for the negative mode; capillary temperature 350 °C; nitrogen gas as sheath and auxiliary gas at pressures of 35 and 15 psi, respectively; capillary voltage −50 V for the negative mode. MS/MS spectra were obtained by data-dependent acquisition (DDA) using collision-induced dissociation (CID).

Microscopic observation and Raman analysis

Digital micrographs were acquired using a three-dimensional digital microscope VHX-5000 (Keyence, Japan) with magnifications between 250 and 2500×. For the cross-sectional observation, sample K4 was embedded in epoxy resin, and then sanded and polished.

Scanning electron microscopy and energy-dispersive X-ray spectroscopy (SEM-EDS) was carried out with a S-3700N tungsten filament scanning electron microscope (Hitachi, Japan) and an energy dispersive X ray spectrometer (Oxford, England). Before the inspection, the cross-sections of samples were sprayed with gold using a high-speed sputter-coating instrument connected with a conductive sheet. The accelerating voltage was set at 20 kV and the working distance was 15 mm.

Raman analysis was performed using a Nova2S Raman spectrometer (Ideaoptics, Shanghai, China) and a BX-43 confocal microscope (Olympus, Tokyo, Japan) with excitation at 532 nm. The laser power applied to the samples ranged between 1 and 3 mW. The Raman spectra were acquired using a 50× objective lens, a spectral range of 86–2986 cm^{-1}, and a resolution of 8 cm^{-1}. The signal was integrated twice, with each collection lasting 8–16 s.

Results

Textile samples

UPLC-PDA-MS analysis showed that all the textiles investigated contained laccaic acids A ($[M-H]^-$ = m/z 536.08), B ($[M-H]^-$ = m/z 495.06), C ($[M-H]^-$ = m/z 538.06) and E ($[M-H]^-$ = m/z 494.07), indicating the use of lac dye as colorant[23] (Table 2). The identification of lac dye in the red yarn sampled from the Yingpan woolen socks (Y1, dated to CE 140 ± 30) represents so far the earliest evidence of the use of lac dye in Xinjiang (Fig. 3a). In a previous study[8], three red dyes including cochineal, lac dye, and dyer's madder (*Rubia tinctorum L.*) were simultaneously identified in a single woolen yarn from a pair of embroidered woolen boots excavated from the Niya site (95MNM3:53), which is dated to the 2nd–3rd centuries CE.

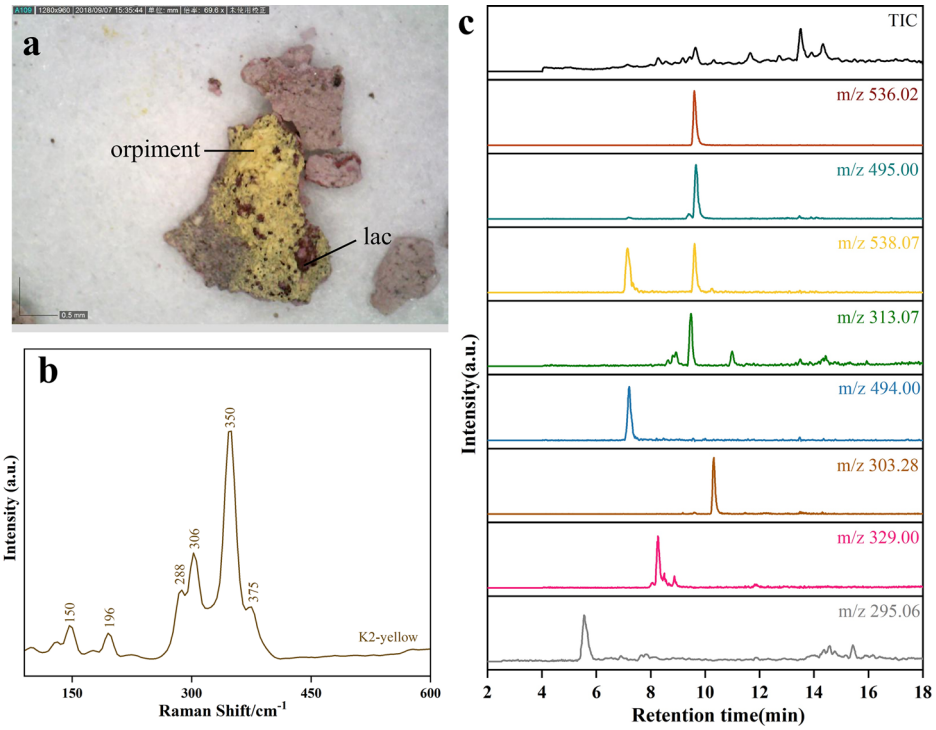

Fig. 4 | The experimental data of sample K2. **a** Microscopic picture. **b** Raman spectrum of yellow pigment (orpiment). **c** Total ion chromatogram (TIC) and extract ion chromatograms (EICs) of the main components by UPLC-PDA-MS analysis (negative mode).

Table 3 | List of compounds identified in the samples collected from Kizil and Simsim Grottoes, and Astana Tombs by UPLC-PDA-MS (negative ion mode)

Possible compounds	Chemical formula	Calculated mass [M-H]-	MS/MS ESI (-) fragment ions	R.T. (min)	K1	K2	K3	K4	S1	S2	S3	S4	A1	A2	A3
Laccaic acid A	$C_{26}H_{19}NO_{12}$	536.08	518.03, 492.13, 448.11	9.5	+	+			+		+	+	+	+	+
Laccaic acid B	$C_{24}H_{16}O_{12}$	495.06	476.98, 451.09, 407.19	9.6	+	+			+		+	+	+	+	+
Laccaic acid C	$C_{25}H_{17}NO_{13}$	538.06	520.02, 494.13, 439.28, 402.20, 365.96	6.4, 9.6		+					+	+	+		+
Laccaic acid D	$C_{16}H_{10}O_7$	313.03	293.00, 269.05, 244.75	9.4, 11.2		+	+	+		+	+		+	+	+
Laccaic acid E	$C_{24}H_{17}NO_{11}$	494.07	476.26, 450.15, 405.22	6.5, 9.7		+								+	+
Aleuritic acid	$C_{16}H_{32}O_5$	303.21	285.14, 267,16, 201.11, 171.10, 155.08, 127.01	10.4	+	+	+	+	+	+	+	+	+	+	+
Kermesic acid	$C_{16}H_{10}O_8$	329.03	283.07, 270.66, 211.26, 187.10, 155.03, 139.93	7.9	+	+	+	+	+	+	+	+	+	+	+
Shellolic acid	$C_{15}H_{20}O_6$	295.12	277.12, 251.01, 249.00, 233.19, 207.05	5.6		+	+	+			+	+	+	+	+

Retention times (R.T.), calculated masses of the deprotonated molecules [M-H], chemical formulas and accurate masses of the fragment ions present in the MS/MS spectra are reported.

Laccaic acids were also found in the other analyzed textiles, which are dated to a later period, between the 6th and 9th century CE: the pink yarn (A4) from the Astana Tomb, the woolen thread (MR1) from the Miran tomb, and the Sogdian robe lining silk samite with horses' roundels (MC1) discovered around Gansu or Qinghai province (Fig. 3b–d).

Wall painting samples

Previous studies generally reported that the grotto wall paintings in the Kucha region of Xinjiang were mainly painted with mineral pigments, such as cinnabar or red lead[24]. However, in this study two red areas (K2 and K3) sampled from cave 171 of the Kizil Grottoes indicated the use of an organic colorant which was taken from a pink-hued Buddha face (Figs. 2f and 4a), overlaid on yellow orpiment pigment, as identified by Raman analysis (Fig. 4b). Laccaic acids A, B, C, D and E, were detected, along with a small amount of kermesic acid ($[M\text{-}H]^-$ = m/z 329.03)[25], demonstrating the presence of lac colorant (Fig. 4c). In addition to these representative compounds, non-colored shellac resin components, such as aleuritic acid ($[M\text{-}H]^-$ = m/z 303.21) and shelloic acid ($[M\text{-}H]^-$ = m/z 295.12)[20,26], were observed in relatively high amounts with UPLC-PDA-MS (Fig. 4c). The presence of lac was also confirmed in four samples taken from the Simsim Grottoes dated between the 5th and 9th centuries CE. All these samples retained shellac resin components, including aleuritic acid and shellolic acid. Laccaic acids A-E were partially detectable due to the varying aging degrees of these colorants (Table 3).

In Buddhist art, small layers of metal leaf (such as gold, silver or tin) were usually overlaid on painted areas to give Buddha a 'shining' appearance[20,27,28]. This gilding technique was quite common in the Kizil and Simsim Grottoes. Samples K4 and S1 were taken from metal foil layers, as indicated in Fig. 2. Analytical examination of sample K4 confirmed that this comprises a top thin layer of gold foil (Fig. 5), combined with a purplish red

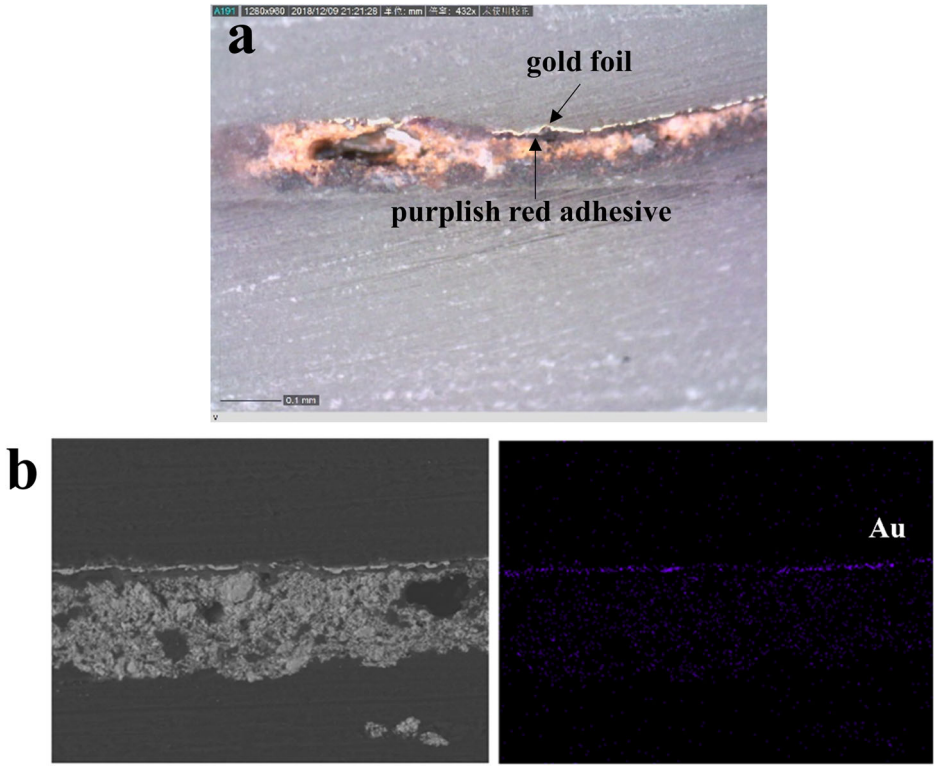

Fig. 5 | The experimental data of sample K4. Top: **a** Cross-sectional micro-photograph highlighting the layers of gold and lac dye-based adhesive; bottom: **b** SEM image (left) and EDS elemental map for gold (right).

resinous substance of lac colorant and shellac (Table 3). These results illustrate a versatile variety of techniques for using lac in wall paintings, not only as red colorant but also as means for gilding.

Sculpture samples

In the purplish red color sculptures (Fig. 2b, c) excavated from the Astana Tombs, lac dye components were furthermore detected (Table 3). The preservation of this organic pigment owes primarily to the incredibly dry and stable environment of the burial chambers, which contributed for the preservation of many sculptures' paint materials.

Discussion

Lac is composed of wax (6–7%), red chromophores known as laccaic acid A-E (4–8%) and resin (70–80%), which consists mainly of terpenic acids, aleuritic acid and several minor fatty acids[29]. Due to the water-solubility of laccaic acid A-E, a lac-dye is prepared by extracting the red chromophores with water-based solvents to produce pure deep red dye[30]. However, in the analyses of the wall paintings from the Kizil and Simsim Grottoes and the painted figurines from the Astana Tombs, both the red pigment and shellac resin components were present, not only as red colorant but also as means for gilding.

Therefore, a rational conjecture is that the shellac components are left on purpose in the formulation of lac pigment in this context. A similar scenario is found in European medieval illuminated manuscripts, where the inclusion of resinous components in lac lake pigment was a desirable feature, as they offered improved binding properties and added sheen to the paint layers[31,32]. It has also been observed in joint investigations of Cave 85 at the Mogao Grottoes (9th-10th century CE) by the Getty Conservation Institute and the Dunhuang Academy Institute, as well as in the wall paintings of Cave 254 at the Mogao Grottoes, that lac might be applied as a red colorant overlaying red minerals to enhance color[33,34].

Lac has a long history as a natural dye. As described in a 1st century CE manuscript, lac was traded as a commodity, '*lakkos chromatinos*', together with cotton cloth from India into the eastern Mediterranean region[35], and it has been identified as a pigment on 3rd century BCE Greek polychromy[36]. In China, the first record of lac can be found in *WuLu* (吴录), written by Zhang Bo during the Jin Dynasty (4th century CE)[37]. However, as shown in this study, lac dye present in the red yarns found in the Yingpan (Y1) and Niya (95MNIM3:53) sites around the Taklamakan Desert demonstrates that lac was brought into Xinjiang at least from the 2nd century CE. Whether lac was brought into the region in the form of dyestuff (which was then applied in local textiles), or already present as a colorant in imported textiles, is impossible to ascertain without a proper study of the origins of the extant textile fragments.

Trade routes connecting India and China, and passing through Xinjiang, were established during the Han Dynasty, promoting the circulation of a wealth of products along the Silk Roads, namely Indian cotton and Chinese silk[38]. Indeed, cotton cloth imprinted with an Indian Buddhist design has been found near the Niya site in Xinjiang, suggesting a close communication between India and Xinjiang during the Han Dynasty[39]. In the following centuries, lac dye and dyed textiles continued to be traded into Northwest China. For example, many relics containing lac dye have been found at archeological sites such as Astana, Miran, and Dunhuang, showing the wide application of this dye in the region[10,34].

Lac dye was used not only for coloring textiles, but also as a pigment in Buddhist architecture. The earliest identification of lac in Buddhist wall paintings was found in samples from Cave 2 (built around CE 450–500) of the Ajanta Grottoes[40], one of the most representative ancient Indian Buddhist cultural sites. Lac glaze was also confirmed in the Nako monastery (11th–12th century CE) in northern India, which was one of the primary Buddhist centers in the western Himalayas[27]. Furthermore, it is speculated by Dhar that a shellac-based coating was probably applied in the Maitreya temple of Basgo in Ladakh[41]. Lac was also found in the Buddhist grotto wall paintings in the Kucha area (Xinjiang) and at Dunhuang (Gansu). By contrast, other insect-derived red colorants, such as kermes and cochineal, have not been observed so far in wall paintings or other painted surfaces of archeological objects from Northwest China, but only on textiles, with identification of these colorants becoming very sporadic in textiles dating after the 3rd century CE[11,42].

It may be possible to interpret the broad use of lac in Buddhist wall paintings, in opposition to the scant finding of kermes and cochineal. As introduced earlier, the extraction process of lac adheres to the basic Buddhist concept of 'non-killing', whereas the production of kermes and cochineal contradicts this ethos.

Furthermore, in Indian culture, there are records about lac in the *Atharva Veda* written around 1500 BCE, one of the earliest Indian religious sacred texts, where lac was highly praised as 'sister of gods' and 'the shining one' for its medicinal value[43]. This implies that lac already had religious connotations since ancient times. Lac was also appreciated for its excellent dye properties since the end of the Vedic period, and was regarded as one of the *eight major colorants* described in Buddhism sutras [1].

Therefore, an interesting interpretation can be given about lac having a strong relation with artistic Buddhist practices. In opposition, kermes and cochineal are absent in Buddhist wall paintings, and are infrequently found in textiles from the 5th to the 10th century CE. For example, no Dunhuang textile (7th to 10th century CE) has so far revealed the presence of kermes or cochineal, while lac dye was identified in various textiles[8–11].

This possibility strengthens the link between the spread of Buddhism and the adoption of lac dye in Northwest China. Indian Buddhism was introduced into Xinjiang in the 1st century BCE. The creation of Buddhist grottoes first emerged in the Kucha area, where the Kizil and Simsim Grottoes are located, and was an important center of Buddhist culture in Xinjiang. This study confirms that lac was used both as red colorant and/or as a gilding adhesive in the Kizil and the Simsim Grottoes. The caves decorated with lac were built in the flourishing period of Buddhism in the Kucha area (after the 5th century CE). Furthermore, the discovery of lac dye in the painted sculptures unearthed from Astana Tombs suggests that the prevalence of Buddhism in ancient Gaochang may have promoted the use and spread of imported Indian products, such as lac dye. In this context, Shevchenko et al. reported the findings of sesame oil and cattle ghee imported from South Asia in connection with Buddhist cultural items unearthed from the Astana Tombs, and have proposed a close correlation between the development of sesame agriculture and the expansion of Buddhism[44]. Therefore, it is conceivable that besides accelerating the integration of religious ideas, the prosperity of Buddhism also led to cultural and artistic exchanges between ancient India and the Western regions of China, and may as well have contributed to the large-scale application of lac in wall paintings.

Data availability

The author confirms that all data generated or analyzed during this study are included in this published article. Furthermore, primary and secondary sources and data supporting the findings of this study are also available online (https://data.mendeley.com/datasets/7wxgykb78c/1).

Received: 14 June 2025; Accepted: 14 October 2025;
Published online: 30 October 2025

References

1. Cardon, D. Vermilion, scarlet and crimson: scale insect sources of anthraquinone dyes. In *Natural Dyes-Sources, Tradition, Technology and Science* 607–666 (Archetype Publications, 2007).
2. Przewoźna, K. S. The history of red in Poland: Polish cochineal *Porphyrophora polonica* and other natural dyes. In *Colour Culture Science* (eds. Godyń, M., Groborz, B. & Lubańska, K. A.) 34–41 (Faculty of Industrial Design, 2018).
3. Donkin, R. A. The insect dyes of western and west-central Asia. *Anthropos* **72**, 847–880 (1977).
4. Gibson, A. J. The story of lac. *J. R. Soc. Arts* **90**, 319–335 (1942).
5. Koren, Z. C. Archaeological shades of purple from flora and fauna from the Ancient Near East. In *Archaeological Chemistry-A Multidisciplinary Analysis of the Past* (eds. Orna, M. V. & Rasmussen, S. C.) 256–300 (Cambridge Scholars Publishing, 2020).
6. Böhmer, H. & Karadag, R. New dye research on Palmyra textiles. *Dyes Hist. Archaeol.* **19**, 88–92 (2003).
7. Gulmini, M. et al. The "Coptic" textiles of the "Museo Egizio" in Torino (Italy): a focus on dyes through a multi-technique approach. *Archaeological Anthropological Sci. Archaeol. Anthr. Sci.* **9**, 485–497 (2017).
8. Liu, J. et al. Profiling by HPLC-DAD-MSD reveals a 2500-year history of the use of natural dyes in Northwest China. *Dyes Pigm* **187**, 109143 (2021).
9. Kramell, A. E. et al. A multi-analytical techniques based approach to study the colorful clothes and accessories from mummies of Eastern Central Asia. *J. Archaeol. Sci. Rep.* **10**, 464–473 (2016).
10. Tamburini, D. Investigating Asian colourants in Chinese textiles from Dunhuang (7th-10th century AD) by high performance liquid chromatography tandem mass spectrometry - Towards the creation of a mass spectra database. *Dyes Pigm* **163**, 454–474 (2019).
11. Hofenk de Graaff, J. H. & Bommel, M. R. Dyestuff analysis of the central Asian woollen textiles. A contribution of dyestuff analysis to the study and knowledge of the textiles fragments. *Riggisberge Ber.* **10**, 137–148 (2001).
12. de Barros Damgaard, P. et al. 137 ancient human genomes from across the Eurasian steppes. *Nature* **557**, 369–374 (2018).
13. Li, Y. Agriculture and palaeoeconomy in prehistoric Xinjiang, China (3000–200 bc). *Veg. Hist. Archaeobot.* **30**, 287–303 (2021).
14. Betts, A. V. G. et al. *The Cultures of Ancient Xinjiang, Western China: Crossroads of the Silk Roads* (Archaeopress, 2019).
15. Liu, S. et al. Silk Road glass in Xinjiang, China: chemical compositional analysis and interpretation using a high-resolution portable XRF spectrometer. *J. Archaeol. Sci.* **39**, 2128–2142 (2012).
16. Liu, J. et al. Characterization of dyes in ancient textiles from Yingpan, Xinjiang. *J. Archaeol. Sci.* **40**, 4444–4449 (2013).
17. Polosmak, N. V., Karpova, E. V. & Amosov, E. V. An unusual fabric from Jety-Asar-2, Eastern Aral Sea region, in the context of the central Asian textile tradition. *Archaeol. Ethnol. Anth.* **48**, 50–58 (2020).
18. Chen, T. et al. Plant use in the Lop Nor region of southern Xinjiang, China: archaeobotanical studies of the Yingpan cemetery (~25–420 AD). *Quatern. Int.* **426**, 166–174 (2016).
19. Zhao, S. et al. Revealing ancient yellow colorants in painted artworks along the silk Road (6th-10th century AD). *J. Archaeol. Sci.* **169**, 106039 (2024).
20. Zhou, Z. et al. Identification of organic materials used in gilding technique in wall paintings of Kizil Grottoes. *Chemistryselect* **5**, 818–822 (2020).
21. Gao, Y. et al. Pigments, dyes and the restoration history of the painted figurines of the Tang Dynasty from the Astana Tombs revealed by comprehensive chemical analysis. *Chemistryselect* **7**, e202202342 (2022).
22. Sheng, P. et al. Foodways of the medieval Tibetans on the Silk Road: new evidence from the Miran Site in Xinjiang. *Holocene* **33**, 91–100 (2023).
23. Ferreira, E. S. B., Hulme, A. N., McNab, H. & Quye, A. The natural constituents of historical textile dyes. *Chem. Soc. Rev.* **33**, 329–336 (2004).
24. Schmidt, B. A. et al. Technical analysis of a Central Asian wall painting detached from a Buddhist cave temple on the northern Silk Road. *Stud. Conserv.* **61**, 113–122 (2016).
25. Lech, K. & Fornal, E. A mass spectrometry-based approach for characterization of red, blue, and purple natural dyes. *Molecules* **25**, 3223 (2020).
26. Tamburini, D., Dyer, J. & Bonaduce, I. The characterisation of shellac resin by flow injection and liquid chromatography coupled with electrospray ionisation and mass spectrometry. *Sci. Rep.* **7**, 14784 (2017).
27. Bayerová, T. Buddhist wall paintings at Nako Monastery, North India: changing of the technology throughout centuries. *Stud. Conserv.* **63**, 171–188 (2018).

28. Gill, M. S., Rendo, C. P. & Menon, S. Materials and techniques: early Buddhist wall paintings and sculptures at Sumda Chun, Ladakh. *Stud. Conserv.* **59**, 300–313 (2014).
29. Santos, R. et al. HPLC-DAD-MS analysis of colorant and resinous components of lac-dye: a comparison between Kerria and Paratachardina genera. *Dyes Pigm.* **118**, 129–136 (2015).
30. Hofenk de Graaff, J. H. *The Colourful Past: Origins, Chemistry and Identification of Natural Dyestuffs* (Archetype Publications, 2004).
31. Berbers, S. V. J., Tamburini, D., van Bommel, M. R. & Dyer, J. Historical formulations of lake pigments and dyes derived from lac: a study of compositional variability. *Dyes Pigm.* **170**, 107579 (2019).
32. Castro, R., Miranda, A. & Melo, M. Interpreting lac dye in medieval written sources: new knowledge from the reconstruction of recipes relating to illuminations in Portuguese manuscripts. In *Sources on Art Technology: Back to* Basics (eds. Green, S. E. et al.) 88–99 (Archtype Publications, 2016).
33. Wong, L. & Agnew, N. *The Conservation of Cave 85 at the Mogao Grottoes, Dunhuang: A Collaborative Project of the Getty Conservation Institute and the Dunhuang Academy* (Getty Publications, 2014).
34. Bolong, C. et al. Virtual reconstruction of the painting process and original colors of a color-changed Northern Wei Dynasty mural in Cave 254 of the Mogao Grottoes. *Herit. Sci.* **10**, 164 (2022).
35. Warmington, E. H. *The Commerce between the Roman Empire and India* (Cambridge University Press, 1931).
36. Dyer, J., Tamburini, D. & Sotiropoulou, S. The identification of lac as a pigment in ancient Greek polychromy - the case of a Hellenistic oinochoe from Canosa di Puglia. *Dyes Pigm.* **149**, 122–132 (2018).
37. Wang, J. The exploitation and use of Butea Gum in Ancient China. *China Hist. Mater. Sci. Technol.* **21**, 222–227 (2000).
38. Dale, S. F. Silk Road, Cotton Road or. Indo-Chinese Trade in Pre-European Times. *Modern Asian Stud*. **43**, 79–88 (2009).
39. Gao, H. *Chinese Textile Designs* (Viking Adult, 1992).
40. Shimadzu, Y. Painting materials and techniques of the Ajanta Wall Paintings. In Conservation and Painting Techniques of Wall Paintings on the Ancient Silk Road (eds. Agnew, N. et al.) 137–156 (Springer, 2021).
41. Dhar, S. Documentation and emergency treatment of Wall Paintings in the Chamba Lakhang (Maitreya Temple): Developing a methodology to conserve Mural Paintings in India's Ladakh district. In *Proceedings of the Second International Conference on the Conservation of Grotto Sites* (ed. Angew, N) 286–296 (The Getty Conservation Institute, 2010).
42. Dusenbury, M. M. & Bethe, M. *Color in Ancient and Medieval East Asia* (Yale University Press, 2015).
43. Karpova, E. et al. Xiongnu burial complex: a study of ancient textiles from the 22nd Noin-Ula barrow (Mongolia, first century AD). *J. Archaeol. Sci.* **70**, 15–22 (2016).
44. Shevchenko, A. et al. Open sesame: identification of sesame oil and oil soot ink in organic deposits of Tang Dynasty lamps from Astana necropolis in China. *PloS One* **12**, e0158636 (2017).

Acknowledgements

This research was supported by the National Key R & D Program of China (2019YFC1520300, 2019YFC1521300), the Bureau of International Cooperation, Chinese Academy of Sciences (131C11KYSB20190035), and the Fundamental Research Funds for the Central Universities and National Social Science Fund (Grant Number: 19BKG045). We would like to give special thanks to Prof. Richard Laursen from Department of Chemistry, Boston University, for valuable comments and careful modification of this manuscript. We also thank Prof. Jisheng Xie, Prof. Ruilei Wang from Zhejiang University and Prof. Shujing Wang from Peking University for their discussion with us on Buddhism art style and archaeology in Central Asia.

Author contributions

Sihan Zhao: Formal analysis, Methodology. Juan Zhang: Formal analysis, Methodology, Writing - original draft. Ana Albano Serrano: Validation, Writing - review & editing. Diego Tamburini: Validation, Writing - review & editing. Xiaojing Kang: Investigation, Resources. Zhibo Zhou: Investigation, Resource, Writing - review & editing. Yumin Gao: Investigation, Resource. Ling Shen: Investigation. Jiakun Wang: Formal analysis. Jie Yang: Investigation, Resource. Shaowen Shi: Methodology, Validation. Jian Liu and Hui Zhang: Conceptualization, Funding acquisition, Resources, Supervision, Writing – review & editing.

Competing interests

The authors declare no competing interests.

Additional information

Correspondence and requests for materials should be addressed to Jian Liu or Hui Zhang.

Reprints and permissions information is available at http://www.nature.com/reprints

Publisher's note Springer Nature remains neutral with regard to jurisdictional claims in published maps and institutional affiliations.

Open Access This article is licensed under a Creative Commons Attribution-NonCommercial-NoDerivatives 4.0 International License, which permits any non-commercial use, sharing, distribution and reproduction in any medium or format, as long as you give appropriate credit to the original author(s) and the source, provide a link to the Creative Commons licence, and indicate if you modified the licensed material. You do not have permission under this licence to share adapted material derived from this article or parts of it. The images or other third party material in this article are included in the article's Creative Commons licence, unless indicated otherwise in a credit line to the material. If material is not included in the article's Creative Commons licence and your intended use is not permitted by statutory regulation or exceeds the permitted use, you will need to obtain permission directly from the copyright holder. To view a copy of this licence, visit http://creativecommons.org/licenses/by-nc-nd/4.0/.

© The Author(s) 2025

Journal of Archaeological Science 169 (2024) 106039

Contents lists available at ScienceDirect

Journal of Archaeological Science

journal homepage: www.elsevier.com/locate/jas

Revealing ancient yellow colorants in painted artworks along the silk Road (6th-10th century AD)

Sihan Zhao [a,1], Zhang He [b,1], Yumin Gao [c,1], Zhibo Zhou [d], Zhiwei Ge [e], Zhenzhen Yang [f], Jing Yan [b], Jie Yang [d,**], Hui Zhang [a,g,*]

[a] School of Art and Archaeology, Zhejiang University, Hangzhou, 310028, PR China
[b] Shaanxi Provincial Institute of Archaeology, Xi'an, 710054, PR China
[c] Xinjiang Uygur Autonomous Region Museum, Urumqi, 830002, PR China
[d] Conservation and Restoration Department, The Kucha Academy of Xinjiang, Urumqi, 830000, PR China
[e] Analysis Center of Agrobiology and Environmental Sciences, Zhejiang University, Hangzhou, 310058, PR China
[f] Conservation and Archaeology of Cultural Relics Department, Luoyang Polytechnic, Luoyang, 471099, PR China
[g] Laboratory for Art and Archaeology Image, Zhejiang University, Hangzhou, 310028, PR China

ARTICLE INFO

Original content: The LC-MS original data (Original data)

Keywords:
Yellow colorant
Wall paintings
Mass spectrometry
Polychrome figurines
Silk Road

ABSTRACT

A comprehensive analytical protocol was undertaken to elucidate the yellow colorants employed in wall paintings from the Kizil Grottoes, the Taojia Tomb, the Baiyangzhai Tomb, and polychrome figurines from the Astana Tombs, all positioned along the historical Silk Road and dating to the 6th-10th centuries AD. To unequivocally identify these colorants, multi-analytical techniques were deployed, encompassing digital microscopy, scanning electron microscopy coupled with energy-dispersive X-ray spectroscopy (SEM-EDS), X-ray fluorescence spectroscopy (XRF), micro-Raman spectroscopy, and ultra-performance liquid chromatography triple quadrupole time-of-flight mass spectrometry (UPLC-Triple TOF-MS/MS). This comprehensive approach facilitated the unambiguous identification of both inorganic pigments, specifically vanadinite, and plant-derived colorants, including gamboge (*Garcinia* sp.) and Chinese cork tree (*Phellodendron chinense*), within these archaeological artifacts. These findings not only significantly enhance our scientific understanding of the materials and techniques utilized in the creation of these wall paintings and polychrome figurines, but also shed light on the vibrant exchange of materials and technological advancements that flourished along the ancient Silk Road.

1. Introduction

Historically, mineral pigments held dominance in the palettes of artists crafting wall paintings and polychrome figurines. Their vibrant hues and resistance to chemical degradation secured their popularity, exemplified by red lead, cinnabar, hematite, orpiment, atacamite, and azurite (Balandier et al., 2017; Cortea et al., 2020; He et al., 2022). In contrast, organic colorants, predominantly consisting of organic chromophore groups, have garnered less scholarly attention, potentially due to their perceived infrequency in ancient art, susceptibility to fading under light and environmental stressors, and often high production costs demanding specialized techniques. While the inorganic pigments tend to have higher opacity and covering power, making them more suitable for opaque paint applications, the organic colorants are often more transparent and can be used to create glazes or semi-transparent layers in paintings. Additionally, the identification of organic materials frequently necessitates sophisticated analytical techniques operating at the molecular level, further hindering a complete understanding of these materials. However, recent research paints a different picture, revealing the continuous use of organic colorants like madder, indigo, and Tyrian purple in diverse mediums, including wall paintings, polychrome terracottas, and painted marble (Bracci et al., 2019; Coccato et al., 2021, Gagliano Candela et al., 2019; Holakooei et al., 2020; Karapanagiotis et al., 2013; Pelosi et al., 2016; Pinto et al., 2018; Sabatini et al., 2016).

* Corresponding author. School of Art and Archaeology, Zhejiang University, Hangzhou, 310028, PR China.
** Corresponding author.
E-mail addresses: 674830093@qq.com (J. Yang), huizhang@zju.edu.cn (H. Zhang).
[1] These authors contributed equally to this work.

https://doi.org/10.1016/j.jas.2024.106039
Received 13 March 2024; Received in revised form 23 July 2024; Accepted 24 July 2024
Available online 27 July 2024
0305-4403/© 2024 Elsevier Ltd. All rights are reserved, including those for text and data mining, AI training, and similar technologies.

Furthermore, discoveries of kermes, lac, and gamboge in artwork suggest a wider and more nuanced application of organic colorants than previously assumed (Bayerová, 2018; Dyer et al., 2018; Osticioli et al., 2019).

In our previous research (Gao et al., 2022; Zhou et al., 2020), indigo blue was found on the painted figurines from the Astana Tombs (3rd-9th century AD), a public cemetery for officials and civilians of the ancient Gaochang Kingdom, and lac dye was detected as the red colorant, while shellac was used as the mordant for gold gilding on the murals of Kizil Grottoes (3rd-9th century AD), the earliest and most westerly grottoes group in China, located on the northern edge of the Taklamakan Desert. These findings suggest a widespread use of organic pigments in ancient artwork. However, the identification of yellow organic pigments has been relatively limited. This is attributed to several factors, including the potential instability of certain yellow pigments for painting applications and the greater analytical challenges associated with their non-invasive identification compared to red and blue pigments (Aceto, 2021). To address this knowledge gap, this study focuses specifically on the analysis of yellow organic pigments, delving into the complexities of their identification and providing a comprehensive evaluation. In the East, yellow traditionally symbolizes kingship, absolute authority and Buddha's benevolence, making its use in artworks particularly significant (Lee et al., 2023). Ancient Chinese artists and craftsmen drew upon a diverse palette of yellow mineral pigments, including yellow ochre (FeOOH), pyrite (FeS_2), pararealgar (As_4S_4), orpiment (As_2S_3) and massicot (PbO) for their visual impact and cultural connotations (Guo et al., 2023; Li et al., 2009; Ma et al., 2023; Sun et al., 2022; Wang et al., 2014).

While numerous plants offer vibrant yellow dyes extensively used in textile dyeing (Abu-Ghosh et al., 2023; Liu et al., 2013; Tamburini, 2019), the presence of yellow lakes identified in painted artifacts through scientific analyses is relatively rare. Notable examples of known yellow lakes include (*Reseda luteola*), gamboge (*Garcinia* sp.), Indian yellow, turmeric (*Curcuma longa*) and buckthorn berries (*Rhamnus* spp.) (Aceto, 2021; Holakooei et al., 2018; Jorge-Villar et al., 2018; Nyström, 2015; Perry et al., 2011; Tamburini et al., 2018). The identifying and characterizing existing yellow organic colorants presents significant challenges. Shared chromophores like luteolin and kaempferol across different dye sources complicate differentiation. Additionally, the inherent light, oxygen, and heat sensitivity of glycoside-flavonoid dyes fosters degradation through photo-oxidation (Ferreira et al., 2004). Furthermore, variations in plant flavonoid characteristics arise based on diverse factors like utilized plant parts, cultivation stages, and environmental conditions (Abu-Ghosh et al., 2023).

Given the intricate composition of painted artworks involving both inorganic and organic compounds such as pigments, binders, and fillers, the use of an integrated strategy with multiple analytical methods becomes essential. Firstly, the identification of mineral pigments is necessary. Currently, Raman spectroscopy, X-ray fluorescence spectroscopy (XRF), scanning electron microscopy equipped with energy-dispersive X-ray spectroscopy (SEM-EDS) are the primary analytical methods for pigment identification in cultural heritage (Pendleton et al., 2014; Perez-Pueyo et al., 2009; Wang et al., 2020). Among these techniques, Raman spectroscopy provides reliable molecular structure information, while XRF and SEM-EDS allow for elemental composition analysis.

High-performance liquid chromatography-mass spectrometry (HPLC-MS) has established itself as the preeminent tool for identifying organic colorants. Its meticulous and comprehensive analysis of organic materials allows for the precise separation and characterization of multi-colored components within dyestuff extracts (Liu et al., 2013; Tamburini, 2019). Driven by technological advancements, ultra-performance liquid chromatography triple quadrupole time-of-flight mass spectrometry (UPLC-Triple TOF-MS/MS) has emerged as an even more powerful technique. Utilizing data-independent acquisition (DIA), this methodology generates both full-scan MS spectra and MS2 spectral data of the analytes, leading to significant improvements in sensitivity and resolution (Yuan et al., 2024).

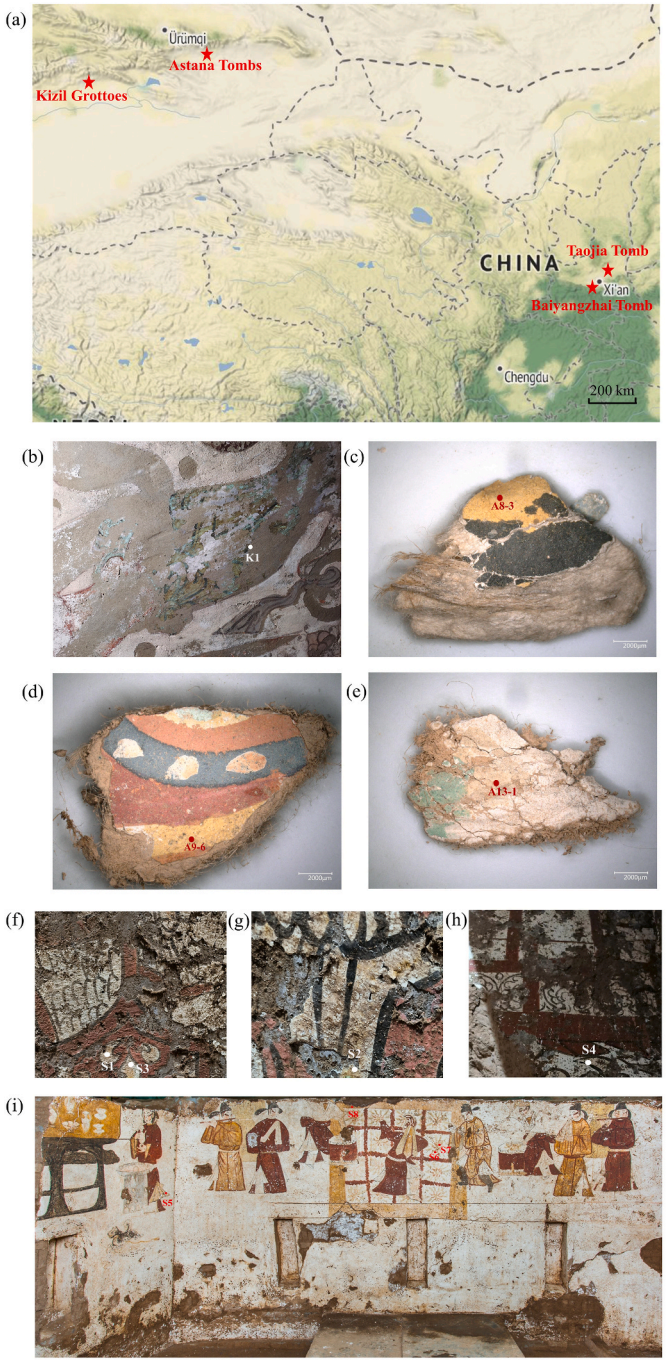

Fig. 1. (a) Geographic location of the Kizil Grottoes, the Astana Tombs, the Taojia Tomb and the Baiyangzhai Tomb. Sampling locations of (b) K1, (c) A8-3, (d) A9-6, (e) A13-1, (f) S1, S3, (g) S2, (h) S4, (i) S5, S6, S7 and S8.

This study investigates the utilization of yellow colorants in murals and painted figurines across key Silk Road sites (Fig. 1a). We specifically focus on the Kizil Grottoes' murals, the Astana Tomb's painted figurines, and the unearthed murals from the Taojia(陶家) Tomb (7th century AD) and Baiyangzhai(白杨寨) Tomb (8th-10th centuries AD) in Shaanxi Province. These tombs, located near the Tang Dynasty capital and serving as the final resting places of powerful ministers Wenzhen Duan and Xingshen Liu, respectively, offer valuable insights into the region's vibrant cultural heritage.

Employing a multi-analytical approach, we start with techniques like

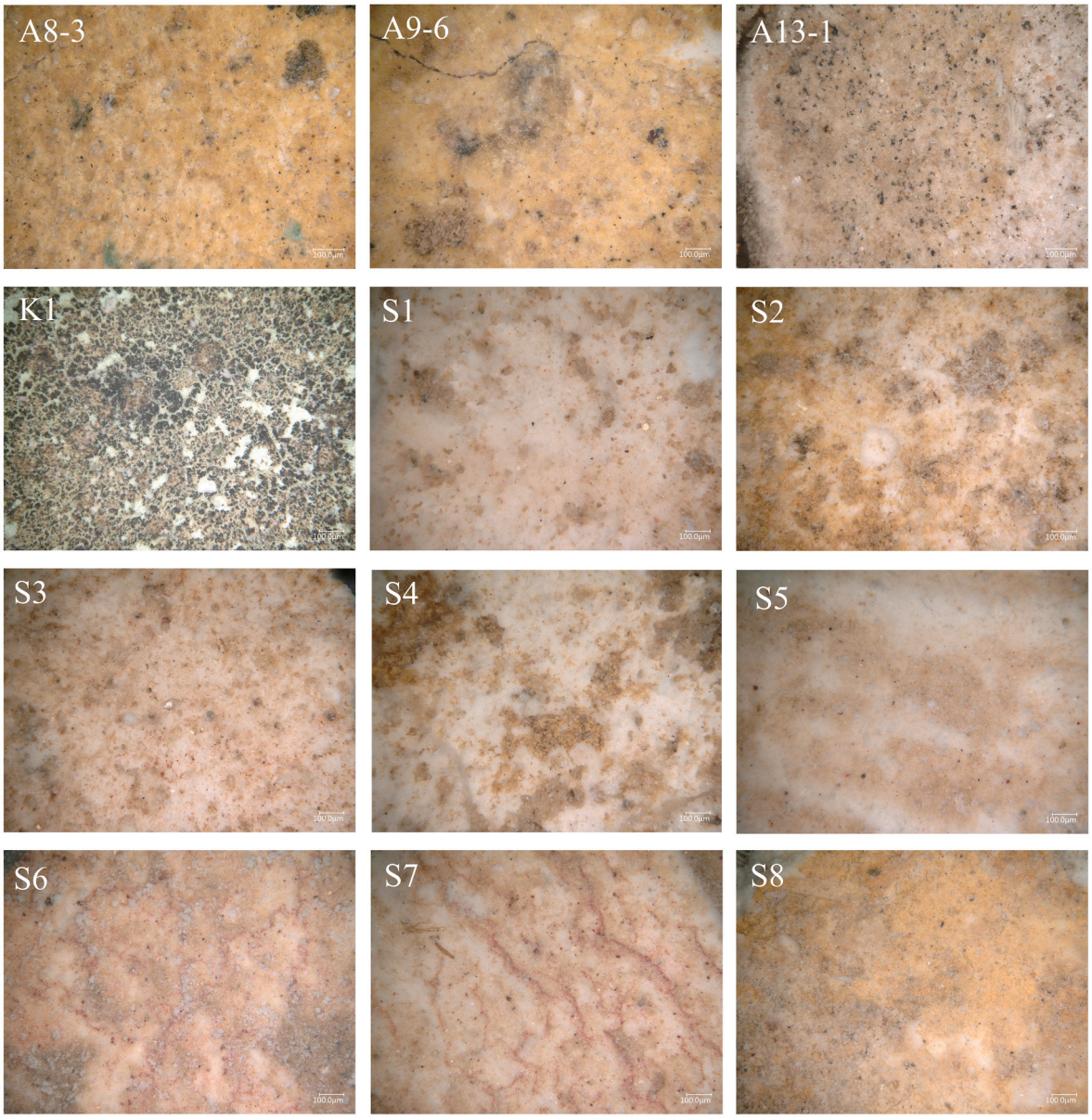

Fig. 2. Digital micrographs of the samples (A8-3, A9-6, A13–1, K1, S1, S2, S3, S4, S5, S6, S7 and S8) used in this study.

microscopy, XRF, SEM-EDS, and Raman spectroscopy. For samples suggesting organic colorants, UPLC-Triple TOF-MS/MS provides further in-depth characterization. Identifying the choice of colorants (inorganic or organic, local or imported) offers valuable insights into trading practices and social life during this historical period. Our investigation, therefore, holds significant potential to enrich our understanding of both art history and cultural communication along the Silk Road.

2. Experimental samples and Instrumentation

2.1. Archaeological samples

Nine yellowish fragments were extracted from mural paintings across the Kizil Grottoes, Taojia Tomb, and Baiyangzhai Tomb, while three additional samples originated from polychrome figurines unearthed at the Astana Tombs (Table S1). Notably, a prior study comprehensively analyzed all colorants within samples A8 and A9 (Gao et al., 2022), excluding only the yellow pigments, which constitute the focus of this investigation. The sampling locations corresponding to these samples are presented in Fig. 1.

2.2. Sample preparation

Sample preparation for cross-sections: Each sample was embedded in 2 × 2 cm molds using TECHNOVIT 2000LC resin. After curing, the embedded samples were subjected to profile grinding using a polisher with a sequential progression of sandpaper grits (1500, 1800, 2400, 3200, 4000, 6000, 8000, and 12000) to achieve a smooth cross-sectional surface.

Extraction for UPLC-Triple TOF-MS/MS: For samples S1, S5, S6, S7, K1, A8-3, A9-6, and A13-1, a dedicated pre-processing protocol was employed. The extraction of colorants was performed using heat-assisted solvent extraction, involving incubation of about 0.1–0.2 mg of each sample with 100 μL of methanol/water (1:1) mixture at 65 °C for 30 min. Subsequent centrifugation at 4000 rpm for 5 min facilitated separation of the extract. Finally, 50 μL of the clarified supernatant was transferred to a 200 μL autosampler vial for UPLC-Triple TOF-MS/MS analysis (Gao et al., 2022).

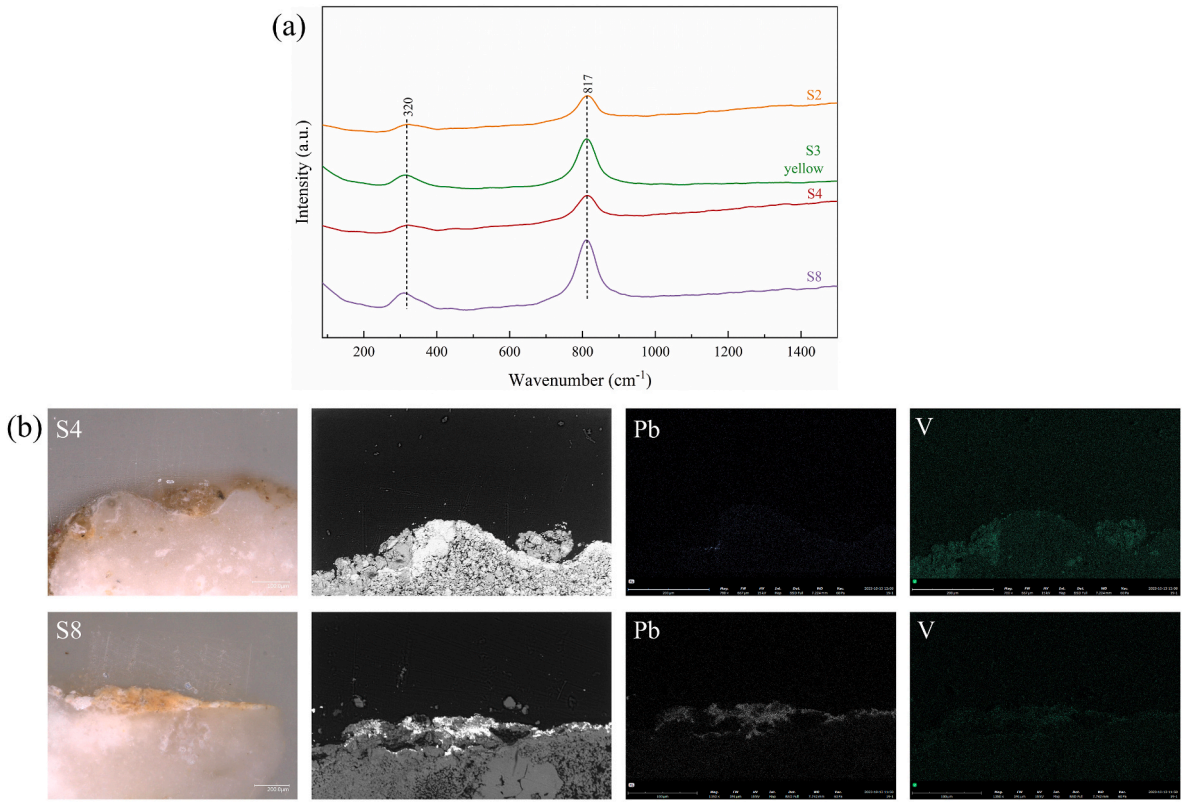

Fig. 3. (a) Raman spectra of yellow pigments from S2, S3, S4 and S8 (b) Images of the cross-sections and element mapping of the archaeological samples S4 and S8. (For interpretation of the references to color in this figure legend, the reader is referred to the Web version of this article.)

2.3. Instrumentation

2.3.1. Digital microscope

A 3D digital VHX-5000 microscope (Keyence, Japan) with magnifications ranging from 20 to 2000 × was used. In areas with significant surface fluctuations, the depth-of-field composite mode was employed.

2.3.2. Scanning electron microscopy and energy-dispersive X-ray spectroscopy (SEM-EDS)

A Phenom XL G2 scanning electron microscope (SEM) combined with a Thermo Fisher Scientific PW-300-021 energy dispersive X-ray spectrometer (EDS) and a backscatter detector were used to analyze the microstructural characteristics of the colorants and to semi-quantify the relative concentrations of major elements in different layers. The analysis was conducted in a low vacuum environment with a pressure of 60 Pa, using a scanning voltage of 15 kV at a working distance of 7 mm.

2.3.3. X-ray fluorescence spectroscopy (XRF)

X-ray fluorescence (XRF) analysis was carried out using an EDX-7000 energy-dispersive X-ray fluorescence spectrometer (Shimadzu, Japan). The instrument was equipped with a rhodium X-ray tube. The X-ray source was operated at 50 kV for the elemental range of aluminum to uranium, and at 15 kV for the range of sodium to scandium. A 1 mm collimator was used, and the analysis time for all samples was 30 s.

2.3.4. Micro-Raman spectroscopy

Raman spectroscopy was performed using a Nova 2 spectrometer from ideaoptics in Shanghai, coupled with an Olympus BX-43 confocal microscope. The laser power applied to the samples ranged approximately between 1 and 3 mW. The Raman spectra reported in this study were acquired using a 532 nm laser as the excitation source, a 50× objective lens, a spectral range of 86–2986 cm^{-1}, and a resolution of 8 cm^{-1}. The signal was integrated twice, with each collection lasting 8–16 s.

2.3.5. Ultra-performance liquid chromatography triple quadrupole time-of-flight mass spectrometry (UPLC-triple TOF-MS/MS)

LC-MS analyses were conducted using a Waters ultra-performance liquid chromatography (UPLC) system, along with an ACQUITY UPLC CSH-C18 column (1.7 μm particle size, 2.1 mm × 100 mm dimensions) from Waters Corporation. The UPLC was coupled to an AB SCIEX TripleTOF 5600plus System mass spectrometer (Framingham, USA). Additional details regarding the instrument conditions are provided in the supporting information.

3. Results and discussion

3.1. Microscopic observation

Microscopic examination (Table S1 and Fig. 2) revealed a brownish-yellow surface with an underlying green pigment layer in samples K1. The Astana Tomb samples (60TAM336) displayed varying shades of yellow: A8-3 and A9-6 were darker, while A13-1 was lighter. Samples from the Shaanxi tombs presented as noticeably faded light yellow with intermingled red particles in S1, S3, S6 and S7, resulting in a pinkish-yellow appearance. Notably, the yellow layers in these samples were relatively thin (Fig. 3b, leftmost column). Interestingly, the cross-sections of S7 revealed minimal red particles and no discernible lamination of pigment layers, suggesting simultaneous mixing rather than distinct overlaying.

3.2. Inorganic pigment analysis

The Raman spectra of the yellow particles in samples S2, S3, S4 and S8 was presented in Fig. 3a, revealing the characteristic bands of vanadinite ($Pb_5(VO_4)_3Cl$) at 320 and 817 cm^{-1}. The band at 320 cm^{-1}

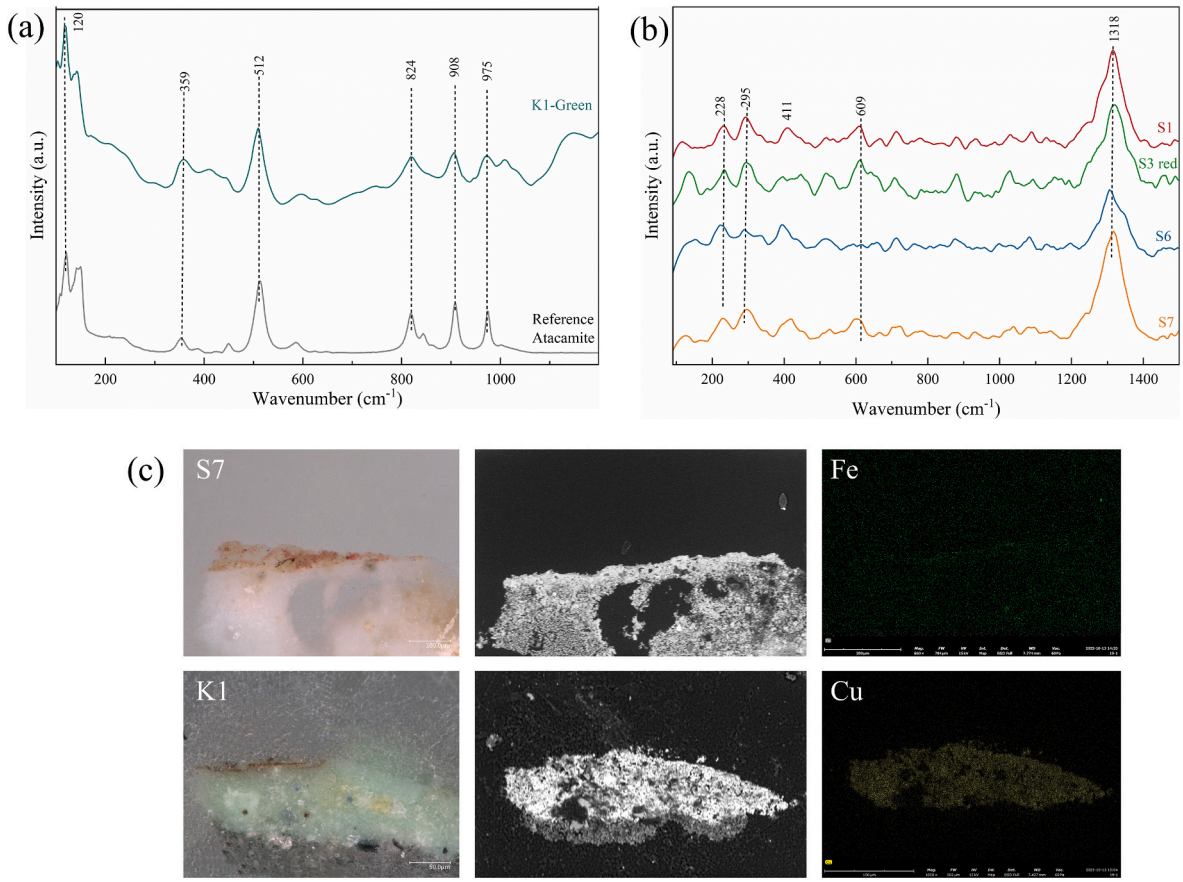

Fig. 4. Raman spectra of (a) green pigments from K1 and reference atacamite (b) red pigments from S1, S3, S6 and S7. Images of the cross-sections and element mapping of (c) S7 and K1. (For interpretation of the references to color in this figure legend, the reader is referred to the Web version of this article.)

was attributed to the degenerate bending vibrations, while the most intense band at 817 cm^{-1} was associated with the degenerate stretching vibrations of VO_4 (Liu et al., 2023). Further confirmation of lead (Pb) and vanadium (V) presence in these samples comes from SEM-EDS and XRF analyses (Fig. 3b and Table S2).

Dating to the Sui and Tang dynasties (7th-10th centuries AD), samples S2, S3, S4, and S8 in this study revealed the use of vanadinite as a yellow pigment. This pigment was also identified in Terracotta Warriors' pottery (Qin Dynasty, 2nd century BC) (Feng et al., 2012), tomb mural paintings from the Western Han Dynasty (206 BCE – AD 25), the Wei and Jin Dynasty (AD 220–420), and the Tang Dynasty (AD 618–906) (Blänsdorf and Yin, 2006; Feng et al., 2012; Guo et al., 2022; Liu et al., 2023; Shui et al., 2020). These findings suggest the use of vanadinite as a yellow pigment throughout the Qin-Tang period (221 BCE to AD 907), primarily within the Shaanxi region.

However, vanadinite detection in painted artifacts beyond Shaanxi, including gothic wall paintings, sinopia, and stucco fragments, indicates its use outside China (Holakooei, et al., 2016, 2018; Levstik et al., 2019; Piovesan et al., 2014). The earliest samples mentioned above can be dated back to the late Sasanian period (AD224–651), later than the Qin Dynasty (2nd century BC), indicating that the vanadium employed in China unlikely originated from Western imports. Furthermore, the discovery of early vanadinite deposits near the Qinling Mountains in Shaanxi strengthens the possibility of local sourcing for this pigment (Guo et al., 2023).

XRF analysis (Table S2) and SEM-EDS data (Fig. 4c) revealed the presence of copper (Cu) and chlorine (Cl) as the dominant elements in the green pigment layer underlying the yellow colorants in samples K1. This finding was corroborated by Raman spectroscopy (Fig. 4a), which identified characteristic bands of atacamite ($Cu_2(OH)_3Cl$). These bands included: 120 cm^{-1} (O-Cu-O bending), 359 cm^{-1} (Cu-Cl stretching), 512 cm^{-1} (Cu-O stretching), and 824, 908, and 975 cm^{-1} (O-H deformation) (De Haro et al., 2023). Collectively, these results demonstrate that the skirt area of the celestial being in Cave 69's rear corridor ceiling (Kizil Grottoes) was first primed with atacamite, followed by outlining the pattern with an organic yellow colorant.

Raman spectroscopy identified hematite (Fe_2O_3) as the red pigment in samples S1, S3, S6 and S7 from the Shaanxi tombs (Fig. 4b). This was confirmed by the characteristic spectrum exhibiting a strong band at 1318 cm^{-1} (collective spin motion) and additional bands at 295, 411, 609 cm^{-1} (Eg modes), and 228 cm^{-1} (A1g mode). (Cerrato et al., 2020). The observed pinkish-yellow hue stems from the combined presence of hematite and yellow colorants like vanadinite or plant-based pigments. Notably, the iron (Fe) content in these samples did not significantly exceed levels found in others, suggesting the use of a limited amount of hematite (Fig. 4c–Table S2).

3.3. Organic colorant analysis

Analysis with a 532 nm excitation laser failed to yield discernible Raman bands in yellow particles from samples S1, S5, S6, S7, K1, A9-6, A13-1, and A8-3. Additionally, XRF analysis detected no chromophore elements, suggesting the presence of organic yellow colorants. For further confirmation, UPLC-Triple TOF-MS/MS was employed.

In sample S1, two compounds exhibiting a measured accurate molecular mass of 342.1716 Da and retention times of 7.5 and 7.8 min in the positive ion mode were identified (Fig. 5, Table 1 and S3). Their secondary mass spectrum displayed major fragmentation peaks at 192.1094, 177.0832 and 148.0789 Da. Based on these features, these two compounds were identified as phellodendrine and magnoflorine

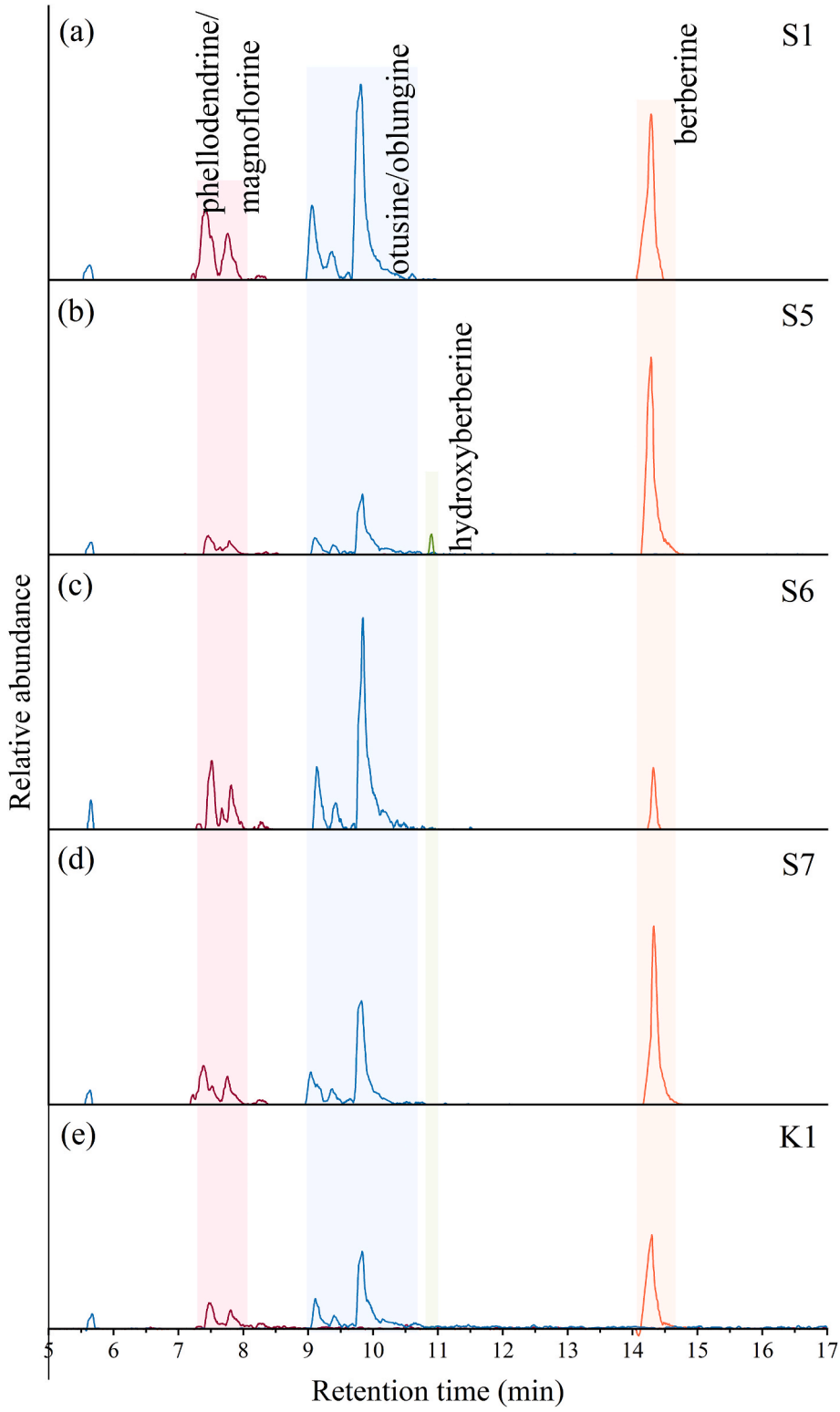

Fig. 5. Extract ion chromatograms of the main components obtained by UPLC-Triple TOF-MS/MS analysis (positive mode) of (a) S1, (b) S5, (c) S6, (d) S7 and (e) K1.

(Tamburini, 2019). Phellodendrine and magnoflorine were also detected in samples S5, S6, S7, K1, A8-3, and A13-1 (Figs. 5 and 6).

Three further high-intensity peaks with retention times of 9.1 and 9.8 min ($[M+H]^+$ = m/z 314.1749), and 14.3 min ($[M+H]^+$ = m/z 336.1229) were observed in the positive ion mode chromatogram. These compounds were identified as lotusine/oblongine and berberine, respectively, based on their accurate relative molecular masses and secondary fragment ions (Tamburini, 2019). Lotusine/oblongine was present in samples S5, S6, S7, K1, A9-6, A13-1, and A8-3, while berberine was found in samples S5, S6, S7, K1, A9-6, A13-1, and A8-3.

Sample S5 displayed a peak at m/z 352.1195 in positive ion mode with a 11.0 min retention time (Fig. 5). Its secondary mass spectrum revealed major fragment ion peaks at 336.0863, 308.0916 and 290.0808. Based on these features, the compound was identified as

Table 1
List of compounds identified in the historical samples by UPLC-Triple TOF-MS/MS (positive ion mode). Retention times (R.T.), calculated masses of the protonated molecules $[M+H]^+$, chemical formulas and accurate masses of the fragment ions present in the MS/MS spectra are reported. The experimental masses of the protonated molecules $[M+H]^+$ are reported in supporting information.

Possible compounds	Chemical formula	Calculated mass $[M+H]^+$	MS/MS ESI (+) fragment ions	R.T. (min)	S1	S5	S6	S7	K1	A8-3	A9-6	A13-1
phellodendrine/ magnoflorine	$C_{20}H_{24}NO_4^+$	342.1700	192.1094, 177.0832, 148.0789	7.5, 7.8	+	+	+	+	+	+		+
lotusine/oblongine	$C_{19}H_{24}NO_3^+$	314.1751	269.1172, 237.0911, 209.0958, 143.0491, 115.0542, 107.0496, 77.0385	9.1, 9.8	+	+	+	+	+	+	+	+
hydroxyberberine	$C_{20}H_{18}NO_5^+$	352.1180	336.0863, 308.0916, 290.0808	11.0		+						
berberine	$C_{20}H_{18}NO_4^+$	336.1230	320.0962, 306.0768, 292.1007, 278.0847, 275.0935	14.3	+	+	+	+	+	+	+	+
forbesione	$C_{28}H_{32}O_6$	465.2272	437.2329, 381.1714, 363.1609, 313.1088, 285.1132, 165.0189	23.8						+	+	
hydroxyneogambogic acid	$C_{38}H_{46}O_{10}$	663.3164	607.2560, 589.2448, 521.1818, 365.0675, 213.0905	24.2						+	+	
morellic acid/isomorellic acid	$C_{33}H_{36}O_8$	561.2483	505.1869, 477.1910, 419.1137, 391.1178, 339.0838, 231. 0654, 213.0910	25.3, 25.4						+	+	+
hydroxygambogic acid	$C_{38}H_{44}O_9$	645.3058	627.2949, 589.2438, 559.2343, 503.1691, 255.1029, 213.0912	25.8						+	+	
neogambogic acid	$C_{38}H_{46}O_9$	647.3215	629.3267, 523.1981, 495.2044, 477.1914, 459.1856, 229.1235	26.2						+	+	
gambogenic acid/ isogambogenic acid	$C_{38}H_{46}O_8$	631.3266	603.3338, 547.2729, 507.2022, 479.2088, 443.1854, 387.1214, 237.0910, 229.1219	26.2,26.5						+	+	
gambogenin/ isogambogenin	$C_{38}H_{46}O_7$	615.3316	491.2075, 463.2125, 367.0809, 297.1137, 207.1001, 83.0490	27.0, 27.1						+	+	
gambogic acid/ isogambogic acid	$C_{38}H_{44}O_8$	629.3109	601.3164, 573.2487, 545.2530, 487.1781, 447.1790, 365.0637, 299.1273, 255.1026, 213.0915	27.2, 27.3						+	+	

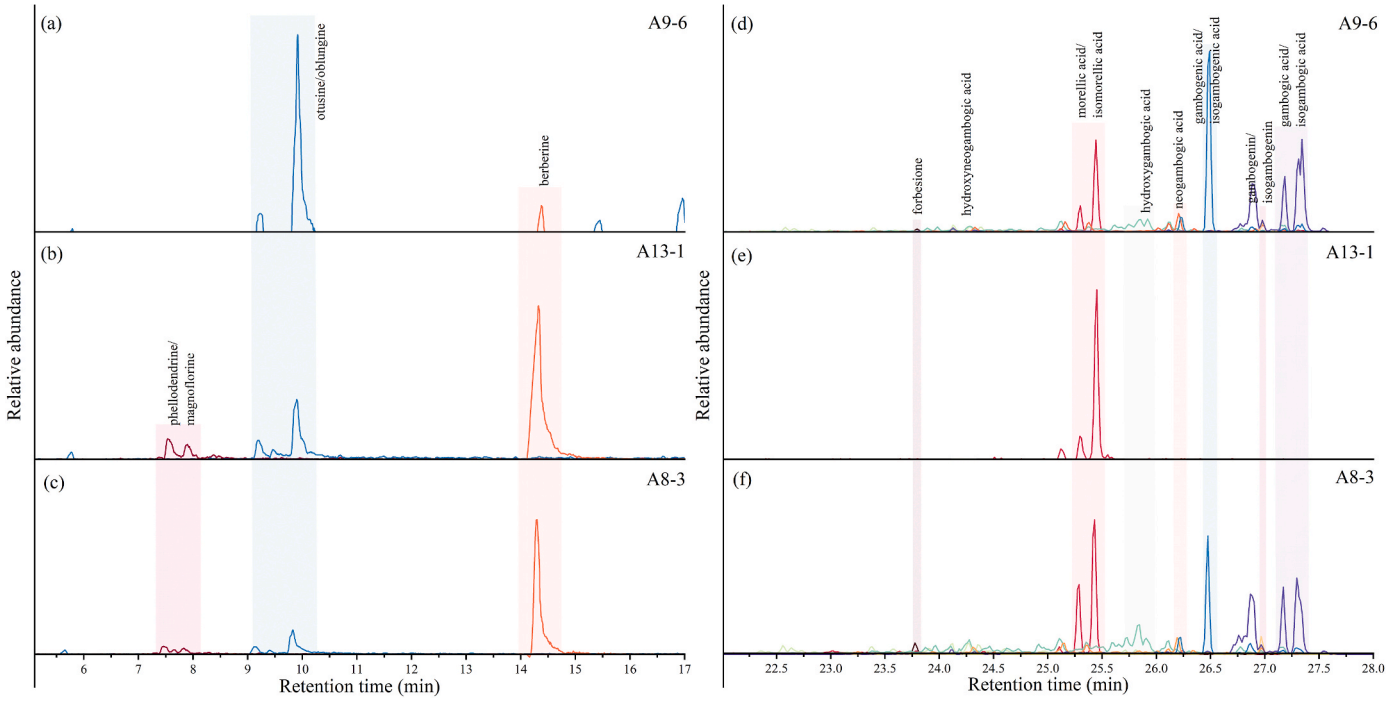

Fig. 6. Extract ion chromatograms of the main components obtained by UPLC-Triple TOF-MS/MS analysis (positive mode) of (a) A9-6, (b) A13-1, (c) A8-3 between 5 and 17min and (d) A9-6, (e) A13-1, (f) A8-3 between 22 and 28 min.

hydroxyberberine (Table 1 and S3) (Tamburini, 2019). The presence of protoberberine alkaloids in these samples confirms the use of colorants derived from *Phellodendron* species.

Plant-based yellow colorants containing protoberberine alkaloids have been widely used in Asia since the Western Han Dynasty (Abu-Ghosh et al., 2023; Han et al., 2017). Common sources include Amur-cork tree (*Phellodendron amurense* in Japan, *Phellodendron chinense* in China), goldthread (*Coptis japonica* in Japan, *Coptis chinense* in China), Japanese barberry (*Berberis thunbergii*), and *huangteng* (*Fibraurea tinctoria*) (Sasaki and Sasaki, 2013). Berberine is the main alkaloid in all these plants except *huangteng* (Zhang et al., 2007). Goldthread is characterized by coptisine, while Amur-cork tree and Japanese barberry contain lower

levels of palmatine and jatrorrhizine compared to berberine. Additionally, Japanese *phellodendron* exhibits a higher palmatine content than the Chinese variety (Sasaki and Sasaki, 2013; Tamburini, 2019). Considering the absence of both palmatine and jatrorrhizine in our results, the yellow pigments in these samples likely originate from Chinese cork tree (*Phellodendron chinense*).

This study constitutes the first to identify Chinese cork tree as a colorant in painted artifacts through scientific analysis. The presence of this tree species in both painted artifacts and textiles from Xinjiang demonstrates its regional accessibility during the studied period and suggests potential transmission from China's Central Plains (Gao et al., 2024; Liu et al., 2013). This finding aligns with reports highlighting significant variations in palmatine content within *Phellodendron* species, emphasizing the need to consider both plant source and potential degradation effects for definitive identification (Sasaki and Sasaki, 2013).

Analysis of yellow samples from the Astana Tombs (A8-3, A9-6, and A13-1) revealed other compounds (Fig. 6, Table 1 and S3). Two peaks with $[M+H]^+$ ions at m/z 629.3116 in sample A8-3 at 27.2 and 27.3 min suggested the presence of gambogic acid and its isomers. Other identified compounds included forbesione, hydroxyneogambogic acid, morellic/isomorellic acid, hydroxygambogic acid, neogambogic acid, gambogenic acid/isogambogenic acid, and gambogenin/isogambogenin, collectively indicating the use of gamboge (*Garcinia* sp.) as a colorant (Tamburini, 2019). Gamboge was also detected in A13–1 and A9-6, leading to the conclusion that all three samples employed a combination of gamboge and Chinese cork tree. Additionally, gamboge had been identified by Raman analysis in a wooden figurine also excavated from the Astana Tombs (Si et al., 2013).

Derived from the bark of *Garcinia* sp. in South and Southeast Asia, gamboge is a yellow gum resin formed from latex secretions that solidifies upon collection. The partially ethanol-soluble resin imparts the yellow hue, while the water-soluble gum remains colorless (Berrie, 2007; Bruni et al., 2011). While the exact historical use of gamboge as a pigment remains unclear, literature cites its mixture with indigo for green hues in traditional Indian murals and its identification in 12th century Indian and 17th-19th century Korean Buddhist paintings (Bayerová, 2018; Lee et al., 2023; Mini, 2010). The tenth-century Tang Dynasty text, "Oversea Materia Medica" (海药本草) by Xun Li (李洵), provides valuable insight into the introduction of foreign medicinal plants to southern China. The work catalogues various imported and transplanted species, including gamboge, also known as "sea gamboge" (海藤). The text notes the growth of gamboge on the cliffs of Ezhou (鄂州) and Yuezhou (岳州), suggesting its cultivation in southern China. Significantly, "Oversea Materia Medica" mentions gamboge's use as a pigment, indicating the emergence of gamboge pigment production within the region during the Tang Dynasty. The presence of gamboge in southern China likely resulted from its introduction from South and Southeast Asia, regions recognized for the natural occurrence of this plant. Therefore, the gamboge pigment discovered in the Astana Tombs may have originated from this source, further underscoring the potential influence of southern China's medicinal trade networks on the development of artistic practices in the region.

The presence of both Chinese cork tree and gamboge, originating from distinct geographical regions, in the Astana Tombs' yellow samples is noteworthy. Similar instances of using multiple colorants from the same color family have been documented in Sogdian silk, potentially for color depth, cost reduction, or enhanced washfastness (Bethe, 2015). This finding highlights the need for further investigation into the rationale behind combining these specific colorants in the Astana Tombs artifacts, opening new avenues for understanding the intricacies of plant-based pigment use in historical artworks. On the other hand, the formation of insoluble lake pigments from water-soluble dyes typically involves precipitation onto a substrate, often aluminum or calcium-based. However, SEM-EDS analysis did not detect the presence of these elements, commonly associated with such substrates, in the analyzed samples. Consequently, definitive conclusions regarding the presence or absence of a precipitation substrate for the organic pigments in this study remain elusive. Future investigations employing more appropriate samples and analytical techniques will be crucial to determine the presence of a substrate and unravel the potential precipitation processes involved in the formation of these organic pigments.

Table 2
List of colorants identified in the archaeological samples considered in this study.

Sample	Mineral pigments detected by XRF, SEM-EDS and Raman spectroscopy	Organic Colorants detected by UPLC-MS
K1	Atacamite	Chinese cork tree
A8-3	–	Gamboge, Chinese cork tree
A9-6	–	Gamboge, Chinese cork tree
A13-1	–	Gamboge, Chinese cork tree
S1	Hematite	Chinese cork tree
S2	Vanadinite	–
S3	Vanadinite, hematite	–
S4	Vanadinite	–
S5	–	Chinese cork tree
S6	Hematite	Chinese cork tree
S7	Hematite	Chinese cork tree
S8	Vanadinite	–

4. Conclusions

This study successfully identified the yellow colorants employed in painted artifacts from the Kizil Grottoes, Taojia Tomb, Baiyangzhai Tomb, and Astana Tombs (Table 2). Notably, three rare yellow colorants were discovered: vanadinite (a mineral pigment) and two plant-based pigments, gamboge (*Garcinia* sp.) and Chinese cork tree (*Phellodendron chinense*). This work marks the first chemical analysis-based confirmation of Chinese cork tree as a colorant in painted artworks, expanding our understanding of the utilization of plant-derived yellow pigments.

Analysis of the experimental data, existing literature, and relevant research suggests that during the 6th-10th centuries AD, vanadinite may have originated locally in northwestern China along the Silk Road, while gamboge could be sourced from Southeast Asia and Chinese cork tree from China's Central Plains. The presence of these colorants in artworks across diverse Silk Road regions illuminates the vibrant trade and material exchange that likely flourished during this era. Particularly noteworthy is the occurrence of two distinct plant-based sources in the Astana Tombs' painted figurines, which could indicate the intricate trade networks and artistic practices at this specific location, though further evidence is needed to confirm these connections conclusively.

Furthermore, this study challenges our established understanding of colorants use in painted artifacts. It reveals the presence of plant colorants alongside the commonly utilized mineral pigments, suggesting that these organic components, often overlooked in painted artifacts, played a significant role in artistic expression. This finding underscores the critical need for increased focus on organic colorants in future research and conservation efforts aimed at preserving murals and painted figurines.

However, further investigation is necessary to fully understand the specific dissemination routes and application processes of these plant colorants. This study provides valuable chemical data that lays the groundwork for exploring the historical use of plant colorants in painted artifacts.

CRediT authorship contribution statement

Sihan Zhao: Writing – original draft, Methodology, Formal analysis. **Zhang He:** Resources, Investigation, Formal analysis. **Yumin Gao:**

Resources, Investigation, Formal analysis. **Zhibo Zhou:** Resources, Investigation, Funding acquisition. **Zhiwei Ge:** Methodology, Funding acquisition. **Zhenzhen Yang:** Resources, Investigation. **Jing Yan:** Resources, Investigation. **Jie Yang:** Resources, Investigation, Conceptualization. **Hui Zhang:** Writing – review & editing, Supervision, Funding acquisition, Conceptualization.

Declaration of competing interest

The authors declare that they have no known competing financial interests or personal relationships that could have appeared to influence the work reported in this paper.

Data availability

The LC-MS original data (Original data) (Mendeley Data)

Acknowledgement

This study was financially supported by National Social Science Fund (Grant Number: 23VJXG024, 19BKG045), the Fundamental Research Funds for the Central Universities and Experimental Technology Research Project of Zhejiang University (szd202104).

Appendix A. Supplementary data

Supplementary data to this article can be found online at https://doi.org/10.1016/j.jas.2024.106039.

References

Abu-Ghosh, S., Sukenik, N., Amar, Z., Iluz, D., 2023. Yellow dyes in archaeological textiles: sources, locations, identification, and challenges. J. Archaeol. Sci.: Reports 49, 104030. https://doi.org/10.1016/j.jasrep.2023.104030.

Aceto, M., 2021. Pigments-the palette of organic colourants in wall paintings. Archaeol. Anthropol. Sci. 13, 159. https://doi.org/10.1007/s12520-021-01392-3.

Balandier, C., Joliot, C., Menager, M., Vouve, F., Vieillescazes, C., 2017. Chemical analyses of Roman wall paintings recently found in Paphos, Cyprus: the complementarity of archaeological and chemical studies. J. Archaeol. Sci.: Reports 14, 332–339. https://doi.org/10.1016/j.jasrep.2017.06.016.

Bayerová, T., 2018. Buddhist wall paintings at nako monastery, north India: changing of the Technology throughout centuries. Stud. Conserv. 63, 171–188. https://doi.org/10.1080/00393630.2017.1327111.

Berrie, B., 2007. Artists' pigments: a handbook of their history and characteristics. Natl. Gallery Art (U.S.) Annu. Rep. 3, 143–153.

Bethe, M., 2015. Color in Ancient and Medieval East Asia. Lawrence, Kansas.

Blänsdorf, C., Yin, X., 2006. A colorful world for the emperor's soul: the polychromy of the terracotta sculptures at Qin shihuang's burial complex. Stud. Conserv. 51, 177–183. https://doi.org/10.1179/sic.2006.51.supplement-2.177.

Bracci, S., Vettori, S., Cantisani, E., Degano, I., Galli, M., 2019. The ancient use of colouring on the marble statues of Hierapolis of Phrygia (Turkey): an integrated multi-analytical approach. Archaeol. Anthropol. Sci. 11, 1611–1619. https://doi.org/10.1007/s12520-019-00803-w.

Bruni, S., Guglielmi, V., Pozzi, F., 2011. Historical organic dyes: a surface-enhanced Raman scattering (SERS) spectral database on Ag Lee–Meisel colloids aggregated by NaClO4. J. Raman Spectrosc. 42, 1267–1281. https://doi.org/10.1002/jrs.2872.

Cerrato, E.J., Cosano, D., Esquivel, D., Otero, R., Jiménez-Sanchidrián, C., Ruiz, J.R., 2020. A multi-analytical study of a wall painting in the Satyr domus in Córdoba, Spain. Spectrochim. Acta A-Mol. Biomol. Spectrosc. 232, 118148 https://doi.org/10.1016/j.saa.2020.118148.

Coccato, A., Mazzoleni, P., Spinola, G., Barone, G., 2021. Two centuries of painted plasters from the Lateran suburban villa (Rome): investigating supply routes and manufacturing of pigments. J. Cult. Herit. 48, 171–185. https://doi.org/10.1016/j.culher.2020.11.010.

Cortea, I.M., Ghervase, L., Tentea, O., Parau, A.C., Radvan, R., 2020. First analytical study on second-century wall paintings from ulpia traiana sarmizegetusa: insights on the materials and painting technique. Int. J. Archit. Herit. 14, 751–761. https://doi.org/10.1080/15583058.2019.1568614.

De Haro, A., Córdova, M., Rua Landa, C., Huck-Iriart, C., Siracusano, G., Maier, M.S., Tomasini, E., 2023. Methodologies for the characterization and identification of natural atacamite as a pigment in andean colonial painting. Herit 6, 5116–5129. https://doi.org/10.3390/heritage6070272.

Dyer, J., Tamburini, D., Sotiropoulou, S., 2018. The identification of lac as a pigment in ancient Greek polychromy - The case of a Hellenistic oinochoe from Canosa di Puglia. Dyes Pigments 149, 122–132. https://doi.org/10.1016/j.dyepig.2017.09.062.

Feng, J., Xia, Y., Blaensdorf, C., Greiff, S., 2012. Analysis on pigments of Western Han Dynasty's tomb mural excavated in the new campus of Xi'an Technology University. J. Northwest For. Univ. 42, 771–776 (in Chinese).

Ferreira, E.S.B., Hulme, A.N., McNab, H., Quye, A., 2004. The natural constituents of historical textile dyes. Chem. Soc. Rev. 33, 329–336. https://doi.org/10.1039/b305697j.

Gagliano Candela, R., Lombardi, L., Ciccola, A., Serafini, I., Bianco, A., Postorino, P., Pellegrino, L., Bruno, M., 2019. Deepening inside the pictorial layers of etruscan sarcophagus of hasti afunei: an innovative micro-sampling technique for Raman/SERS analyses. Mol 24, 3403. https://doi.org/10.3390/molecules24183403.

Gao, S., Yao, M., Narenggaowa, Guo, D., Li, Y., Do, K.L., Liu, J., Zhao, F., 2024. Identification of fibers and dyes in archaeological textiles from Bazhou, Xinjiang (220-420 CE), and their Silk Road origins. J. Archaeol. Sci. 164, 105941 https://doi.org/10.1016/j.jas.2024.105941.

Gao, Y.M., Zhao, S.H., Wang, J.K., Zhou, Z.B., Wan, J., Yang, J., Zhang, H., Zhang, J., 2022. Pigments, dyes and the restoration history of the painted figurines of the Tang dynasty from the Astana tombs revealed by comprehensive chemical analysis. ChemistrySelect 7, e202202342. https://doi.org/10.1002/slct.202202342.

Guo, R., Feng, J., Liu, R., Xia, Y., Fu, Q., Xi, N., Wang, Z., 2022. Rare colour in medieval China: case study of yellow pigments on tomb mural paintings at Xi'an, the capital of the Chinese Tang dynasty. Archaeom 64, 759–778. https://doi.org/10.1111/arcm.12739.

Guo, Z.Y., Cai, S.Q., Zhu, Z.Y., Qin, Y.L., Yao, X.Y., Wang, J., Jin, W.X., Shi, M.F., Li, L.F., Yang, J.C., Liu, L., 2023. Multi-analytical investigation into the materials and techniques of paintings on Northern Wei Dynasty (398-494 CE) coffin planks excavated from Shanxi, China. Humanit. Soc. Sci. Commun. 10, 682. https://doi.org/10.1057/s41599-023-02166-z.

Han, J., Wanrooij, J., van Bommel, M., Quye, A., 2017. Characterisation of chemical components for identifying historical Chinese textile dyes by ultra high performance liquid chromatography – photodiode array – electrospray ionisation mass spectrometer. J. Chromatogr. A 1479, 87–96. https://doi.org/10.1016/j.chroma.2016.11.044.

He, J., Zhou, W.Q., Hu, D.B., Liu, S.J., Otero, J., Rodriguez-Navarro, C., 2022. A multi-analytical approach for the characterization of materials, manufacturing process and damage mechanisms of wall paintings in Samye Temple, Tibet. Dyes Pigments 207, 110704. https://doi.org/10.1016/j.dyepig.2022.110704.

Holakooei, P., de Lapérouse, J.F., Rugiadi, M., Carò, F., 2018. Early Islamic pigments at Nishapur, north-eastern Iran: studies on the painted fragments preserved at the Metropolitan Museum of Art. Archaeol. Anthropol. Sci. 10, 175–195. https://doi.org/10.1007/s12520-016-0347-7.

Holakooei, P., Karimy, A.-H., Hasanpour, A., Oudbashi, O., 2016. Micro-Raman spectroscopy in the identification of wulfenite and vanadinite in a Sasanian painted stucco fragment of the Ghaleh Guri in Ramavand, western Iran. Spectrochim. Acta A-Mol. Biomol. Spectrosc. 169, 169–174. https://doi.org/10.1016/j.saa.2016.06.033.

Holakooei, P., Karimy, A.-H., Saeidi-Anaraki, F., Vaccaro, C., Sabatini, F., Degano, I., Colombini, M.P., 2020. Colourants on the wall paintings of a mediæval fortress at the mount Sofeh in Isfahan, central Iran. J. Archaeol. Sci.: Reports 29, 102065. https://doi.org/10.1016/j.jasrep.2019.102065.

Jorge-Villar, S.E., Rodríguez Temiño, I., Edwards, H.G.M., Jiménez Hernández, A., Ruiz Cecilia, J.I., Miralles, I., 2018. The Servilia tomb: an architecturally and pictorially important Roman building. Archaeol. Anthropol. Sci. 10, 1207–1223. https://doi.org/10.1007/s12520-016-0450-9.

Karapanagiotis, I., Mantzouris, D., Cooksey, C., Mubarak, M.S., Tsiamyrtzis, P., 2013. An improved HPLC method coupled to PCA for the identification of Tyrian purple in archaeological and historical samples. Microchem. J. 110, 70–80. https://doi.org/10.1016/j.microc.2013.02.008.

Lee, N.R., Yun, J.H., Kim, S.J., 2023. Raman spectroscopy of yellow organic pigments of large Korean Buddhist paintings from the late Joseon dynasty (17th–19th centuries). J. Raman Spectrosc. 54, 836–846. https://doi.org/10.1002/jrs.6565.

Levstik, M.G., Mladenovic, A., Kriznar, A., Kramar, S., 2019. A Raman microspectroscopy-based comparison of pigments applied in two Gothic wall paintings in Slovenia. Period. Mineral. 88, 95–104. https://doi.org/10.2451/2019PM778.

Li, T., Xie, Y.F., Yang, Y.M., Wang, C.S., Fang, X.Y., Shi, J.L., He, Q.J., 2009. Pigment identification and decoration analysis of a 5th century Chinese lacquer painting screen: a micro-Raman and FTIR study. J. Raman Spectrosc. 40, 1911–1918. https://doi.org/10.1002/jrs.2340.

Liu, J., Mouri, C., Laursen, R., Zhao, F., Zhou, Y., Li, W.Y., 2013. Characterization of dyes in ancient textiles from Yingpan. Xinjiang. J. Archaeol. Sci. 40, 4444–4449. https://doi.org/10.1016/j.jas.2013.06.034.

Liu, Z., Xu, W., Zhang, Y., Wang, Y., Li, J., 2023. Identification of the pigments on the mural paintings from an ancient Chinese tomb of Tang dynasty using micro-Raman and scanning electron microscopy/energy dispersive X-ray spectroscopy analysis. Miner 13, 1224. https://doi.org/10.3390/min13091224.

Ma, J.J., Li, Y., Wu, F.R., Wang, Y.H., Guo, H., He, X., Zhang, X.T., Wang, F.P., 2023. In situ analysis of pigments on the murals of Yanshan Temple in Fanshi County, Shanxi Province, China by portable Raman and XRF spectrometers. Eur. Phys. J. Plus 138, 48. https://doi.org/10.1140/epjp/s13360-023-03690-2.

Mini, P.V., 2010. Preparation techniques of pigments for traditional mural paintings of Kerala. Indian J. Tradit. Knowl. 9, 635–639.

Nyström, I., 2015. Spectroscopic analysis of artists' pigments and materials used in southern Swedish painted wall hangings from the eighteenth and nineteenth centuries. Stud. Conserv. 60, 353–367.

Osticioli, I., Pagliai, M., Comelli, D., Schettino, V., Nevin, A., 2019. Red lakes from Leonardo's Last Supper and other Old Master Paintings: micro-Raman spectroscopy of anthraquinone pigments in paint cross-sections. Spectrochim. Acta A-Mol. Biomol. Spectrosc. 222, 117273 https://doi.org/10.1016/j.saa.2019.117273.

Pelosi, C., Agresti, G., Andaloro, M., Baraldi, P., Pogliani, P., Santamaria, U., La Russa, M. F., Ruffolo, S.A., Rovella, N., 2016. Micro-Raman and micro-stratigraphic analysis of the forty martyrs in sahinefendi, cappadocia (Turkey). Archaeom 58, 659–672. https://doi.org/10.1111/arcm.12184.

Pendleton, M.W., Washburn, D.K., Ellis, E.A., Pendleton, B.B., 2014. Comparing the detection of iron-based pottery pigment on a carbon-coated sherd by SEM-EDS and by micro-XRF-SEM. Yale J. Biol. Med. 87, 15–20. https://doi.org/10.1017/s143192761401188x.

Perez-Pueyo, R., Soneira, M.J., Castanys, M., Ruiz-Moreno, S., 2009. Fuzzy approach for identifying artistic pigments with Raman spectroscopy. Appl. Spectrosc. 63, 947–957. https://doi.org/10.1366/000370209788964412.

Perry, J.J., Brown, L., Jurneczko, E., Ludkin, E., Singer, B.W., 2011. Identifying the plant origin of artists' yellow lake pigments by electrospray mass spectrometry. Archaeom 53, 164–177.

Pinto, M., Gill, M.S., Georgakopoulou, M., Menon, S., 2018. Examination of 14-15th century Buddhist wall paintings from a cave complex in Saspol, Ladakh. J. Archaeol. Sci.: Reports 21, 259–267. https://doi.org/10.1016/j.jasrep.2018.07.016.

Piovesan, R., Maritan, L., Neguer, J., 2014. Characterising the unique polychrome sinopia under the Lod Mosaic, Israel: pigments and painting technique. J. Archaeol. Sci. 46, 68–74. https://doi.org/10.1016/j.jas.2014.02.032.

Sabatini, F., Lluveras-Tenorio, A., Degano, I., Kuckova, S., Krizova, I., Colombini, M.P., 2016. A matrix-assisted laser desorption/ionization time-of-flight mass spectrometry method for the identification of anthraquinones: the case of historical lakes. J. Am. Soc. Mass Spectrom. 27, 1824–1834. https://doi.org/10.1007/s13361-016-1471-4.

Sasaki, Y., Sasaki, K., 2013. Analysis of Protoberberines in historical textiles: determining the provenance of East Asian textiles by analysis of Phellodendron. e-Preserv. Sci. 10, 83–89.

Shui, B.W., Su, B.M., Yu, Z.R., Cui, Q., Wang, Z., Yin, Z.Y., Shan, Z.W., 2020. Analysis of mimetite-group minerals in mural paintings from the Wei and Jin dynasty tombs of jiayuguan. Dunhuang Res. 1, 133–140 (in Chinese).

Si, Y., Jiang, H.E., Wang, B., He, Q.J., Hu, Y.W., Yang, Y.M., Wang, C.S., 2013. Raman microspectroscopic analysis of polychrome wooden artifact from the Astana tomb of the Tang dynasty, Xinjiang, China. Spectr. Anal. 33, 2607–2611.

Sun, F., Wang, R.S., Liang, Y.X., Liu, J.R., Yao, X., Zhao, F., 2022. Analysis of color paint for moyan stone carvings in shuining temple in bazhong. Spectrosc. Spectr. Anal. 42, 505–511. https://doi.org/10.3964/j.issn.1000-0593(2022)02-0505-07.

Tamburini, D., 2019. Investigating Asian colourants in Chinese textiles from Dunhuang (7th-10th century AD) by high performance liquid chromatography tandem mass spectrometry - towards the creation of a mass spectra database. Dyes Pigments 163, 454–474. https://doi.org/10.1016/j.dyepig.2018.12.025.

Tamburini, D., Martin de Fonjaudran, C., Verri, G., Accorsi, G., Acocella, A., Zerbetto, F., Rava, A., Whittaker, S., Saunders, D., Cather, S., 2018. New insights into the composition of Indian yellow and its use in a Rajasthani wall painting. Microchem. J. 137, 238–249.

Wang, N., He, L., Egel, E., Simon, S., Rong, B., 2014. Complementary analytical methods in identifying gilding and painting techniques of ancient clay-based polychromic sculptures. Microchem. J. 114, 125–140. https://doi.org/10.1016/j.microc.2013.12.011.

Wang, X., Zhen, G., Hao, X., Tong, T., Ni, F., Wang, Z., Jia, J., Li, L., Tong, H., 2020. Spectroscopic investigation and comprehensive analysis of the polychrome clay sculpture of Hua Yan Temple of the Liao Dynasty. Spectrochim. Acta A-Mol. Biomol. Spectrosc. 240, 118574 https://doi.org/10.1016/j.saa.2020.118574.

Yuan, S., Gao, P., Wu, S., Liang, X., Xiao, Y., Tu, P., Jiang, Y., 2024. Rapid and comprehensive metabolites identification of 5-demethylnobiletin in rats using UPLC/Triple-TOF-MS/MS based on multiple mass defect filter and their neuroprotection against ferroptosis. J. Pharm. Biomed. Anal. 238, 115842 https://doi.org/10.1016/j.jpba.2023.115842.

Zhang, X., Corrigan, K., MacLaren, B., Leveque, M., Laursen, R., 2007. Characterization of yellow dyes in nineteenth-century Chinese textiles. Stud. Conserv. 52, 211–220. https://doi.org/10.1179/sic.2007.52.3.211.

Zhou, Z., Shen, L., Li, C., Wang, N., Chen, X., Yang, J., Zhang, H., 2020. Investigation of gilding materials and techniques in wall paintings of Kizil Grottoes. Microchem. J. 154, 104548 https://doi.org/10.1016/j.microc.2019.104548.

Journal of Archaeological Science: Reports 49 (2023) 104061



Contents lists available at ScienceDirect

Journal of Archaeological Science: Reports

journal homepage: www.elsevier.com/locate/jasrep

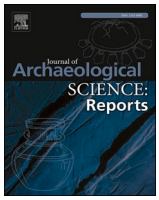



Non-invasive study of the dyes and pigments in the Chinese woodblock *New Year* paintings

Sihan Zhao [a,1], Xiaoyi Jin [b,1], Ling Shen [c], Jin Wang [d], Hanyan Ding [a], Juan Zhang [a], Hui Zhang [a,e,*]

[a] School of Art and Archaeology, Zhejiang University, Hangzhou, China
[b] Crafts Museum of China Academy of Art, Hangzhou, China
[c] Department of Archaeology, Zhejiang University City College, Hangzhou, China
[d] Institute of Yangliuqing New Year Paintings, Tianjin, China
[e] Laboratory of Art and Archaeology Image, Zhejiang University, Hangzhou, China

ARTICLE INFO

Keywords:
New Year paintings
Synthetic colorants
Hyperspectral imaging
MA-XRF
Raman spectroscopy

ABSTRACT

Woodblock *New Year* painting is a traditional Chinese folk art that flourished during the 19th and early 20th centuries. These paintings feature a wide variety of colors, particularly after the introduction of synthetic colorants from Europe in the late 19th century. The scientific identification of dyes and pigments used in these paintings can provide valuable insights into the socio-historical context of the time. However, the history of materials used in the printing of *New Year* paintings is still lacking adequate information. In this study, we employed a combination of spectroscopic and imaging techniques, including Macro X-ray fluorescence imaging (MA-XRF), hyperspectral imaging, and Raman spectroscopy to identify the dyes and pigments used in two Yangliuqing *New Year* paintings. Our analysis revealed the presence of both traditional pigments and synthetic colorants, such as vermilion, Prussian blue, and methyl/crystal violet. We also discovered several color-matching techniques used to create light pink, light orange, and dark purple hues. These findings suggest that synthetic colorants were gradually replacing traditional pigments in China due to the growth of global trade at that time. Furthermore, our research provides valuable information for the conservation, preservation, and display of *New Year* paintings.

1. Introduction

New Year painting, a type of decorative woodblock print for mass consumption, is an ancient Chinese folk art since Tang Dynasty (618–907 CE) (Wang, 2002). These paintings were usually posted on the doors during the Spring Festival to welcome an auspicious start of the *New Year*. The production of *New Year* paintings reached its peak with a development of popular culture during the Qing Dynasty (1644-1912 CE) when there were four major centers of making *New Year* paintings with distinctive styles: Yangliuqing (杨柳青) in Tianjin, Zhuxianzhen (朱仙镇) in Kaifeng, Taohuawu (桃花坞) in Suzhou and Yangjiabu (杨家埠) in Weifang (Pu, 2008; Wang, 2002, 2005).

In East Asia, the introduction of woodblock engraving techniques from China facilitated the creation of folk paintings such as Japanese woodblock prints (also known as *ukiyo-e*), Korean folk paintings, and Vietnamese folk paintings. Like *New Year* paintings, these artworks were produced through woodblock printing, which provided an affordable means of making paintings available to the public (Biron et al., 2020a; oh, 2007; Pyong-Mo, 2006, 2010). In this technique, the underlying drawings are printed in black lines and carved blocks of different colors are created to ensure precise alignment. This allows each color to be printed on a single sheet of paper. Additionally, some hand-applied colors are used in small areas of the paintings (Wan et al., 2019).

Chinese *New Year* paintings embody the cultural characteristics of China, including its customs, beliefs, and aesthetics, and are therefore of significant research value. Previous studies have focused on preserving this folk art as intangible heritage by examining the inheritance of carving and printing techniques (Pu, 2008; Wang, 2002, 2005; Xiao and Wang, 2010). Identifying the materials used in their production can enhance our understanding of the history of art and the creative process

* Corresponding author at: School of Art and Archaeology, Zhejiang University, Hangzhou, China.
E-mail address: huizhang@zju.edu.cn (H. Zhang).
[1] These authors contributed equally to this work.

https://doi.org/10.1016/j.jasrep.2023.104061
Received 23 January 2023; Received in revised form 6 May 2023; Accepted 27 May 2023
Available online 2 June 2023
2352-409X/© 2023 Elsevier Ltd. All rights reserved.

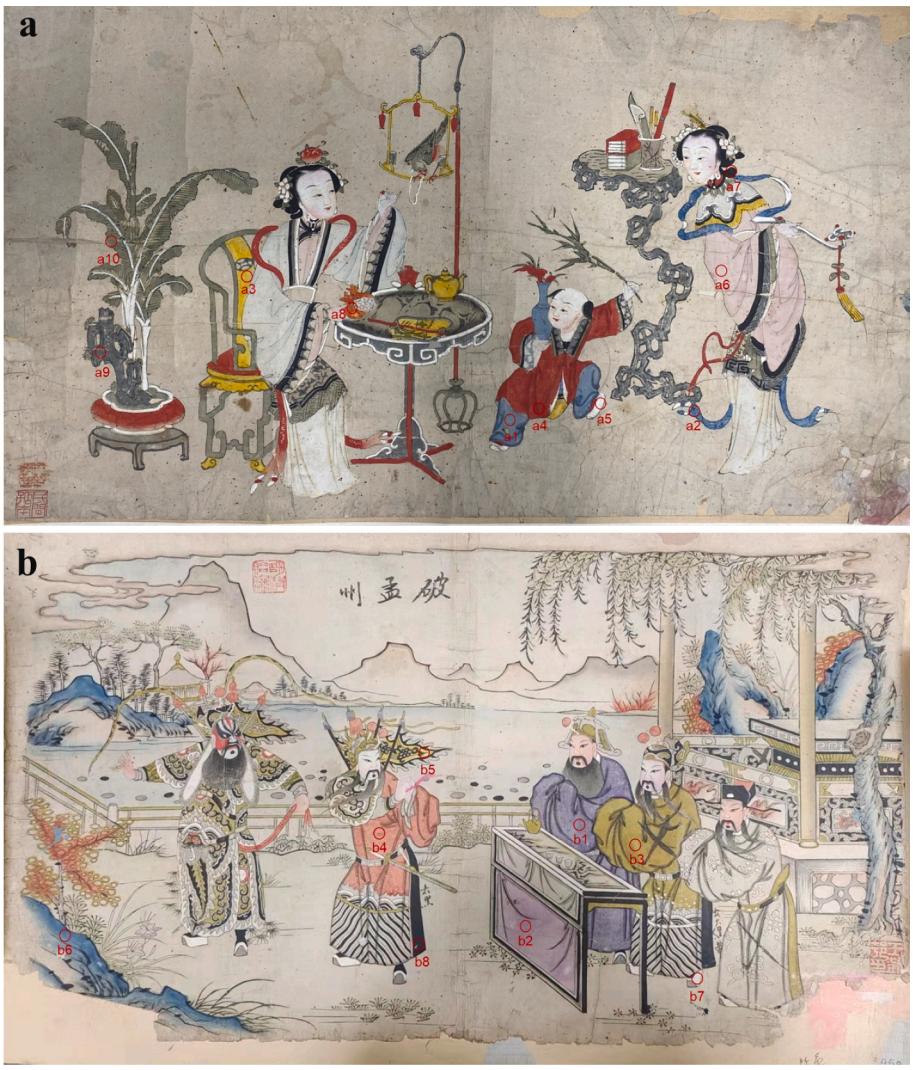

Fig. 1. (a) *A Blessing from Bamboo*, 59 × 34 cm. (b) *Attacking Mengzhou City*, 59 × 34 cm. Studied spots are marked in the paintings with small red circles.

behind *New Year* paintings. The economic, artistic, and technical choices behind these colorants - such as whether they were natural or synthetic, locally sourced or imported - can provide insight into artistic trends and social history. However, to date, there has been little scientific analysis of the dyes and pigments used in the early *New Year* paintings.

Many studies have been conducted to analyze colorants on prints, such as Japanese *ukiyo-e* prints, the artworks of the same period as the *New Year* paintings in China, in which diverse coloring materials (traditional Japanese pigments, plant dyes and synthetic organic colorants) have been identified. (Biron et al., 2018; Biron et al., 2020a; Biron et al., 2020b; Cesaratto et al., 2018; Cesaratto et al., 2019; Edwards and Villafana, 2020; Kissell et al., 2022; Mounier et al., 2018; Perez-Arantegui et al., 2018). In fact, artworks on paper are too precious or too fragile to risk damaging the appearance of the surface of paintings for sampling. Therefore, colorants on woodblock prints generally require non-invasive analytical methods for identification such as Macro X-ray fluorescence imaging technology (MA-XRF), Raman spectroscopy, and hyperspectral imaging.

MA-XRF has become one of the most valuable and useful methods for characterizing the inorganic pigments used in artworks in recent years (dos Santos et al., 2018; Kokiasmenou et al., 2020; Mazzinghi et al., 2021; Saverwyns et al., 2018; Sciutto et al., 2018). MA-XRF builds on XRF by scanning areas point by point and imaging the data to obtain elemental distribution maps, making it easier to associate elements with specific area of interest, and providing detailed information about the pigments used in paint layers and the previous restoration.

Raman spectroscopy is widely used in the field of cultural heritage, which can provide reliable molecular structure information, but it is extremely difficult to identify natural dyes or lakes in *New year* paintings due to their poor Raman scatterers (Stanley, 2015; Tamburini and Dyer, 2019); In addition, the interference generated by the fluorescence emission of the paper increases the background signal and makes the Raman signal hidden. Alternatively, surface-enhanced Raman scattering (SERS) can be used because the enhancement of Raman scattering amplitude solves the problem of identifying very low concentrations of pigments, but not all woodblock prints allow micro-sampling (Cesaratto et al., 2019; Kissell et al., 2022).

Hyperspectral imaging can be regarded as digital imaging coupled with reflectance spectroscopy (Daniel et al., 2016) and is suitable for the in-situ and non-invasive analysis of material studies in artworks, such as paintings (Daniel et al., 2017; de Viguerie et al., 2020), manuscripts (Cucci et al., 2018; de Viguerie et al., 2018), illuminations (Mounier et al., 2016). However, it may be insufficiently selective to allow an accurate discrimination between compounds involved in some mixtures (Cavaleri et al., 2013; Tamburini and Dyer, 2019). Considering that these methods mentioned above provide incomplete information on their own, they are suitable for multi-analytical studies.

In this study, a combination of non-invasive analytical approach, including MA-XRF imaging, hyperspectral imaging in the visible range, and Raman spectroscopy, was conducted on two Yangliuqing *New Year*

paintings to identify the dyes and pigments.

2. Experimental samples and instrumentation

2.1. Historical New Year paintings

Two paintings dated back to late 19th century from the collection of Yangliuqing *New Year* Painting Institute were studied in this work. The first one called "*A Blessing from Bamboo*" (竹报平安, 59 × 34 cm) depicted a scene of a child holding a bamboo branch in his hand and a vase on his arm, while standing next to two women, one of which sitting on a carved chair feeding a parrot, and the other one holding a *ruyi* (如意) (Fig. 1a). This painting expresses the metaphor of best wishes for travel security. The other one, "*Attacking Mengzhou City*" (破孟州, 59 × 34 cm) is based on the classic novel "*Romance of the Sui and Tang Dynasties*". In the scene, Li Shimin wore a king's hat, a yellow robe, and a jade belt across his waist, while Xu Maogong wore a turban and a plum blossom robe on the right and Cheng Yaojin wore a helmet and a purple robe on the left. The three people bade farewell to Qin Qiong and Yuchi Gong who wore armor and back flags, as they were going to attack Mengzhou city (Fig. 1b).

Different colors, including bright yellow, red, blue, pink, green, orange, black and white, are present on "*A Blessing from Bamboo*", while dark purple, red, yellow, blue, black and white can be seen on "*Attacking Mengzhou City*". A few studied spots were selected for further analysis, whose details could be seen in Fig. 1, including the areas and colors they referred to.

2.2. Reference samples

In *New Year* paintings, the three primary colors are red, blue, and yellow. These colors can be combined to produce a range of hues, including purple and green. Our study primarily focused on the colorants stored in the Taohuawu *New Year* Painting Society in Suzhou or those early synthetic colorants which achieved commercial success (Hagan and Poulin, 2021). We also included common natural dyes as reference samples. It is important to note that the colorants used in *New Year* paintings have not been previously identified. Therefore, the inclusion of a reference colorant in our study does not necessarily imply its use in *New Year* paintings, nor does it suggest that our list is exhaustive.

2.2.1. Synthetic colorants

Brilliant Crocein (Acid Red 73, C.I. 27290), Methyl violet (Basic Violet 1, C.I. 42535)/Crystal violet (Basic Violet 3, C.I. 42555), and Metanil yellow (Acid Yellow 36, C.I.13065) were obtained from the Taohuawu *New Year* Painting Society. The actual pigment powders have been confirmed to be consistent with the Color Index numbers labeled above by infrared spectroscopy as shown in Fig. S1 but methyl violet and crystal violet could not be distinguished due to their same spectrum (Zaffino et al., 2017). Auramine O (Basic Yellow 2, C.I. 41000), Victoria blue B (Basic Blue 26, C.I. 44045), and Methylene blue (Basic Blue 9, C.I. 52015) were purchased from Shandong Yousuo Chemical Technology Co., Ltd (China).

2.2.2. Natural dyes

The natural dyes and lakes were made according to the following conventional procedures of making Yangliuqing *New Year* paintings.

Sappanwood (*Biancaea sappan*): Weigh sappanwood and water in a ratio of 1:10, soak overnight, boil the solution and then cool down for 30 min.

Lac (*Kerria lacca*): Weigh smashed stick lac and water in a ratio of 1:20, soak overnight, then heat the solution in water bath at 80 °C for 20 min.

Cochineal (*Dactylopius coccus*): Weigh cochineal and water in a ratio of 1:100, and soak overnight.

Pagoda bud (*Sophora japonica*): Weigh fried and dried pagoda bud and water in a ratio of 1:20, boil the solution and then cool down for 30 min.

Cape jasmine (*Gardenia jasminoides Ellis*): Weigh smashed cape jasmine and water in a ratio of 1:100, soak for 4 h, boil the solution for 20 min.

Turmeric (*Curcuma longa L.*): Weigh turmeric and water in a ratio of 1:10, boil the solution for 30 min.

Amur-cork tree (*Phellodendron amurense Rupr.*): Weigh smashed amur-cork tree and water in a ratio of 1:10, boil the solution and then cool down for 20 min.

Gamboge (*Garcinia hanburyi*): Weigh smashed gamboge and water in a ratio of 1:10, boil the solution for 30 min.

Table S1 showed the structural formulas of the synthetic colorants and the main chemical components of natural dyes which were studied in this work.

2.2.3. Lakes

Pagoda bud lake: Calcium oxide was added to the filtered dye solution while stirring until colorful precipitation appeared.

Other lakes: The dye solution was diluted with water until translucent state, then 2% alum solution was added with the volume ratio of 150:19, the mixed solution was stirred well and stored at room condition for one day. Then the solution was filtered and the resulting precipitate was dried at 45℃. The above process was repeated for several times until the dye solution showed no color.

These lake pigments can be used for painting by adding them directly to the binder (gelatin: water 1:10, adjusted for consistency), and then printed through small wooden blocks on bamboo paper, a type of handmade paper often used in *New Year* paintings, as shown in Fig. S2.

2.3. Instrumentation

2.3.1. Microscopy

AF4515T-FUW portable digital microscope (Dino-Lite, Taiwan) with a magnification of 20–220× and a resolution of 1280 × 1024 pixels was used to observe the microscopic state of paintings *in situ*.

2.3.2. Raman spectroscopy

A Nova 2 spectrometer (ideaoptics, Shanghai), coupled with a BX-43 confocal microscope (Olympus, Tokyo) was utilized for Raman analysis. The laser power ranged approximately between 1 ~ 3 mW on the samples. The Raman spectra reported in this study were acquired with an excitation wavelength of 532 nm laser, an objective lens of 50×, 86 ~ 2986 cm^{-1} spectral range, and a resolution of 8 cm^{-1} by integrating the signal two times for 8 ~ 16 s in each collection.

2.3.3. Macro X-ray fluorescence imaging (MA-XRF)

CRONO X-ray fluorescence analyzer (Bruker, Germany) was utilized for elemental imaging. The scanner is fixed on a motorized stand so that it can be set at any angle for completely non-contact and non-destructive measurements, which are made by a couple of lasers (axial and focal) and a micro-camera allowing up to 600 × 450 mm^2 scanning area and 75 mm focusing axis with the speed up to 42 mm/s. The scan within an area of interest by MA-XRF will build a distribution map of particular elements showing brighter area on the map for higher elemental abundance. The measuring conditions were the following: 50 kV X-ray tube, 200 μA current, 1 mm X-Ray collimators and pixel size, and 30 ms single-pixel time. It took about 32 min to complete the scanning of 237 × 230 mm^2 area on *A Blessing from Bamboo*, and 33 min for the scanning of 280 × 200 mm^2 area on *Attacking Mengzhou City*.

2.3.4. Hyperspectral imaging (HSI)

Reflectance spectra were collected by GaiaField N17E (Dualix spectral imaging) camera with 320 × 256 pixels. The collecting spectrum was ranged from 400 to 1000 nm with the resolution of 5 nm. The paintings were evenly illuminated by two halogen lamps during the

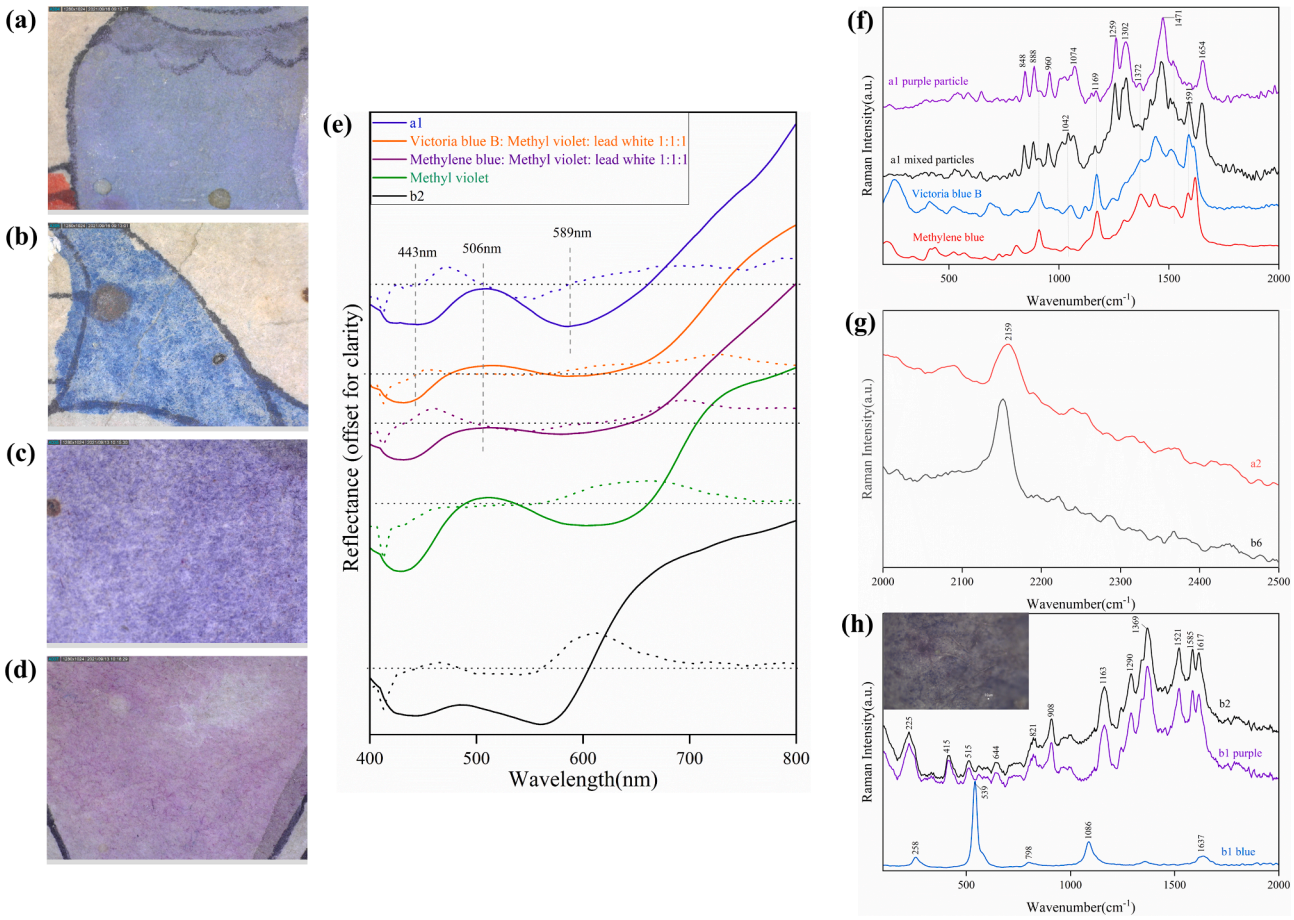

Fig. 2. Micrograph of areas of (a) a1; (b) a2; (c) b1; (d) b2. (e) Reflectance spectra of a1, b2, methyl/crystal violet, Victoria blue B + methyl/crystal violet + lead white, and methylene blue + methyl/crystal violet + lead white. The dashed line of the same color is the first derivative of the reflectance spectrum. Raman spectra obtained for (f) the purple and mixed particles of a1, Victoria blue B and Methylene blue; (g) a2 and b6; (h) the purple and blue particles of b1, respectively, and b2, as well as the micrograph of areas of b1.

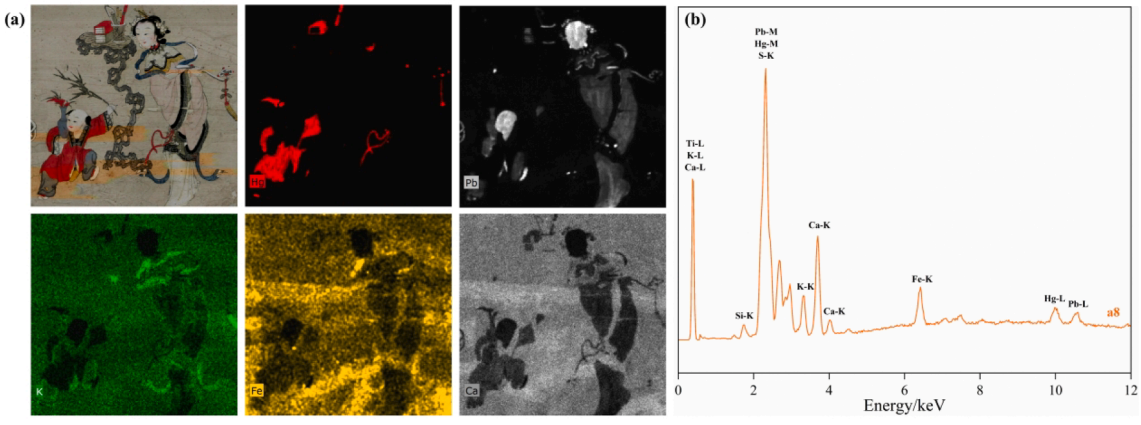

Fig. 3. (a) Selected MA-XRF element maps from an area of *A Blessing from Bamboo*. (b) XRF spectrum of a8.

collecting process and the system was controlled by Spec View software. The obtained data cube was treated with ENVI 5.1 + IDL software. In this study, only the reflectance spectra were considered.

3. Results and discussion

3.1. Blue and purple pigments

The two *New Year* paintings have three tones of blue located in the pants (a1) and the lady's ribbon (a2) in *A Blessing from Bamboo*, and the mountains (b6) in *Attacking Mengzhou City*. Prussian blue ($Fe_4[Fe(CN)_6]_3$) was identified to be used in both the ribbon and the mountains by Raman spectra with a band at 2516 cm^{-1} ascribed to the hexacyanoferrate ions (Fig. 2g) (Edwards and Benoy, 2007), which also explained the high abundance of Fe in both blue areas (Fig. 3 and Fig. 4). Prussian blue was synthesized in 1704 CE, subsequently introduced as a pigment for painters in 1724 CE and was employed in paintings all over Europe by the mid-18th century (Seldes et al., 1999), including some

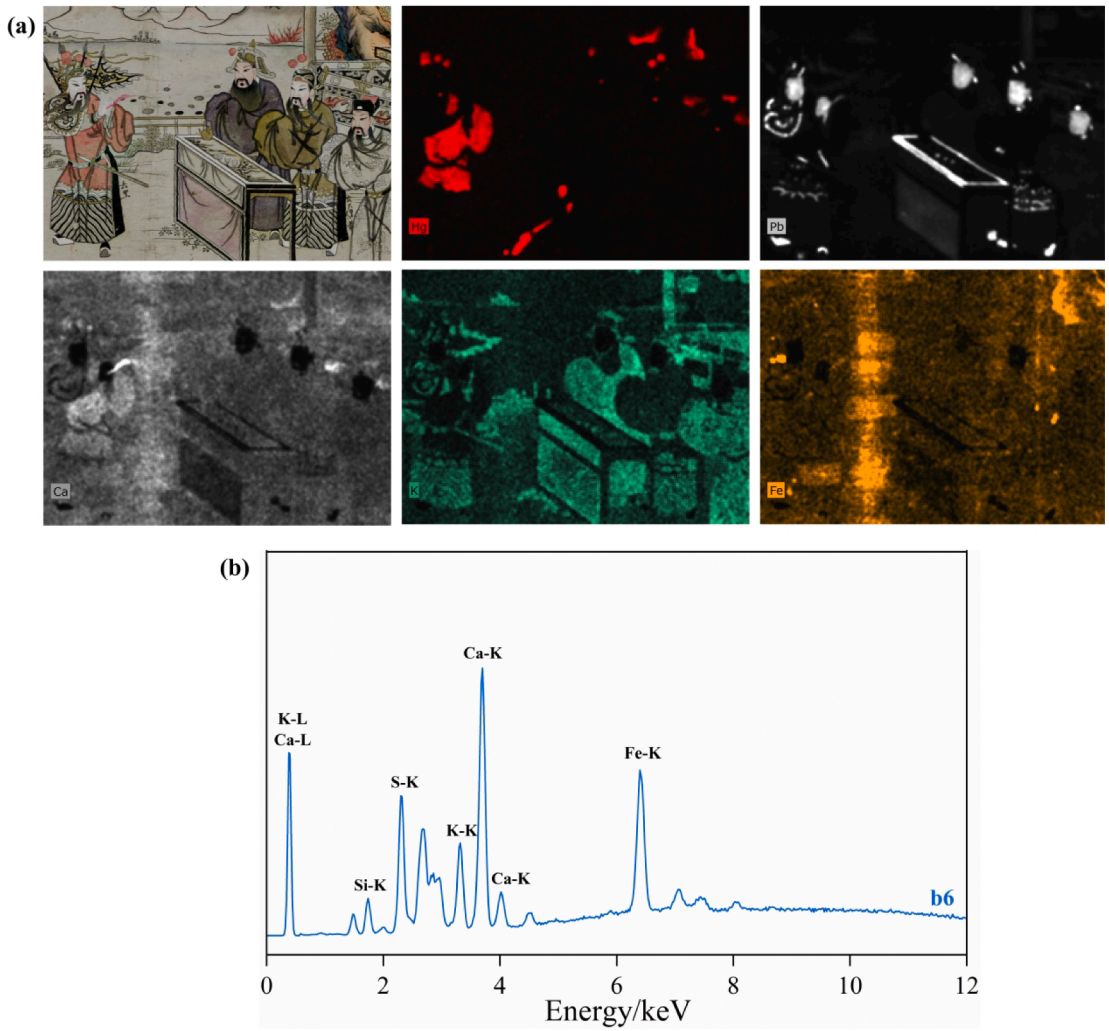

Fig. 4. (a) Selected MA-XRF element maps from an area of *Attacking Mengzhou City*. (b) XRF spectrum of b6.

masterpieces such as *The Starry Night and Starry Night Over the Rhone*. Depending on historical records, the British East India Company began to export Prussian blue from England to China in 1775 CE, and this trade activity continued for several years (Bin et al., 2017).

The pants appeared purple under the microscope (Fig. 2a), probably by mixing two colors. By comparing the Raman spectra obtained by focusing the laser on the purple and blue particles, the peak of 1042 cm^{-1}, 1372 cm^{-1} and 1591 cm^{-1} originated from blue pigments was obtained, probably indicating the presence of Victoria blue B or methylene blue (Fig. 2f). However, the purple pigment didn't correspond to any of the early synthetic purple dyes such as methyl/crystal violet, and it was presumed that the purple may be an anthraquinone dye based on 1471 cm^{-1} (Whitney et al., 2006). In addition, lead (Pb) was found in the pants, suggesting that lead white ($Pb_3(OH)_2(CO_3)_2$) was most likely used with the purple and blue pigments in a mixture to tone down the dark hue in the particular case. Considering the above, two blue pigments, Victoria blue B and methylene blue, were chosen to be mixed with methyl/crystal violet and lead white, respectively, and then the reflectance spectra of a1 was compared with these two reference samples, respectively. The result (Fig. 2e) showed that the three spectra had similar characteristics, with the reflectance minimum bands at 443, 589 nm and the maximum band at 506 nm. Given the lack of sufficient reference materials, this mixed pigment could not be identified and could only be considered as a mixture of organic blue, organic violet and lead white.

There are light purple and dark purple in *Attacking Mengzhou City* as shown in Fig. 2c and Fig. 2d. The dark purple has purple stain marks and blue particles under microscopic observation. The blue particles were confirmed as ultramarine by Raman bands at 258 cm^{-1} (the bending vibration of S_3^-), 539 cm^{-1} (the symmetric stretching vibration of S_3^-), 798 cm^{-1} (the symmetric stretching vibration of Al–O), 1086 cm^{-1} (the anti-symmetric stretching vibration of SO_4^{2-}) as well as 1617 cm^{-1} (harmonic) (Caggiani et al., 2014), while the purple stain marks were confirmed as methyl/crystal violet by Raman bands at 848, 888, 960, 1074, 1169, 1259, 1302, 1372, 1471, 1654 cm^{-1}, which was the same as the Raman spectra of light purple as shown in Fig. 2h. Methyl violet, consisting of a mixture of tetra-, penta- and hexa- methylated pararosaniline, was patented in 1861 and introduced to the market in 1866 (Confortin et al., 2010), while crystal violet was patented in 1883, and their molecular structures are quite similar and cannot be distinguished by Raman spectroscopy (Leona et al., 2011; Zaffino et al., 2017). In addition, methyl/crystal violet was identified in a Japanese woodblock print dated to 1892 (Confortin et al., 2010; Leona et al., 2011; Zaffino et al., 2017). Although the import of methyl/crystal violet into China is not easy to track through overseas trade journals and customs records (He et al., 2019), this result implies that such imported synthetic colorants must have been widely used at that time. Synthetic colorants were also detected in some Chinese paintings of the late 19th and early 20th centuries since they were introduced to China from the West (Kogou et al., 2015; Liu et al., 2019; Zhang et al., 2021).

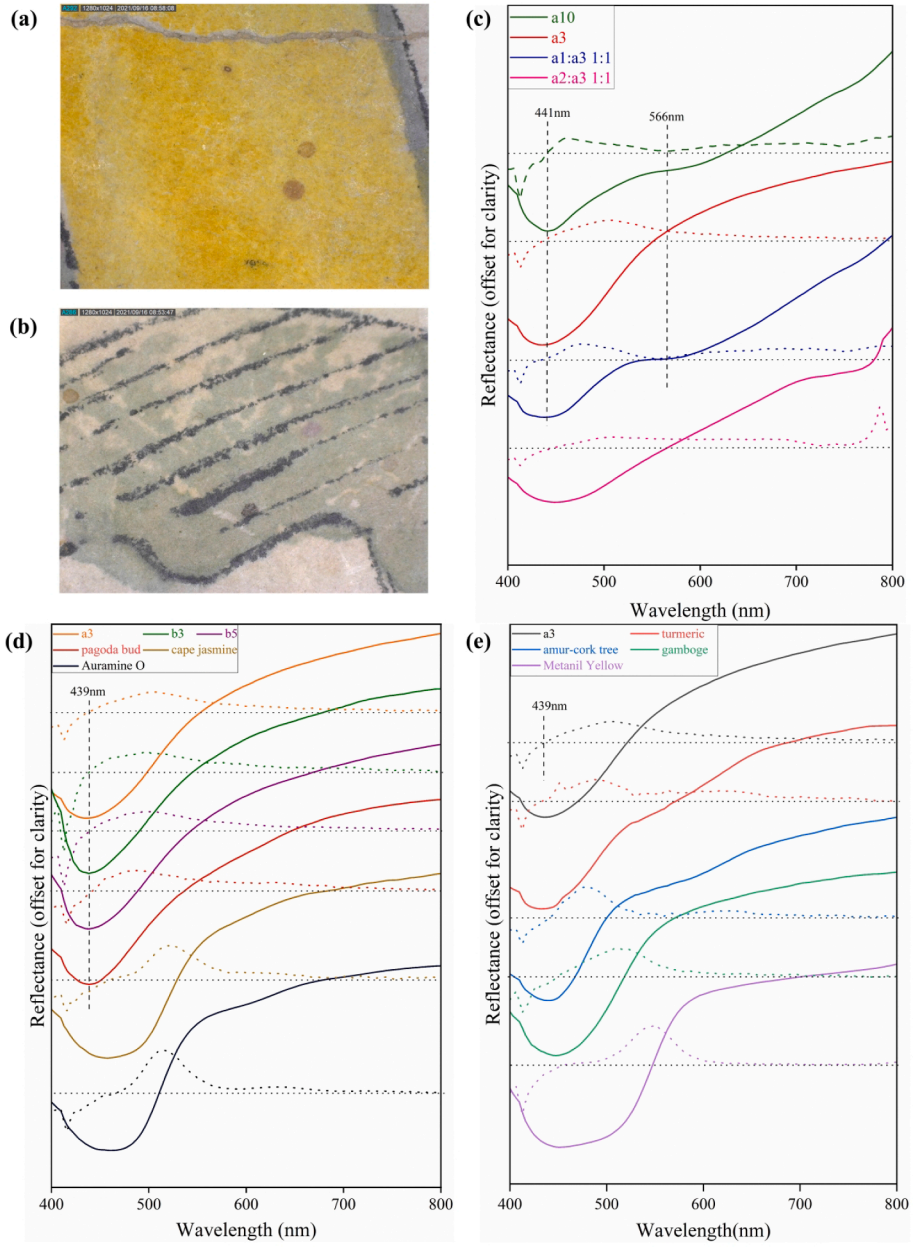

Fig. 5. Micrograph of areas of (a) a3; (b) a10. Reflectance spectra of (c) a3, a10, a1 + a3, a2 + a3; (d) a3, b3, b5, pagoda bud, cape jasmine, and Auramine O; (e) a3, turmeric, amur-cork tree, gamboge, and Metanil yellow. The dashed line of the same color is the first derivative of the reflectance spectrum.

3.2. Yellow and green pigments

Yellow and green pigments were used in many areas in both paintings, such as the chairs (a3) and green leaves (a10) in *A Blessing from Bamboo* as shown in Fig. 5a and Fig. 5b, the robes (b3) and flags (b5) in *Attacking Mengzhou City*. No chromophore elements were detected by XRF method, suggesting organic colorants might be used. To figure out the yellow dyes in these paintings, the reflectance spectra of a1, five traditional yellow dyes, and two synthetic yellow dyes from the hyperspectral imaging were compared. According to Fig. 5d and Fig. 5e, the reflectance curves of a3, b3 and b5 showed consistent characteristics that the apparent maxima of absorption were all located at 439 nm, which was quite similar to pagoda bud, a natural dye derived from the dry flower buds of the *Sophora japonica L.* native to China. Indeed, the non-invasive discrimination of yellow dyes is a challenge because all these dyes were reported to present almost the same spectral characteristics in the visible range, as the absorptions occur mainly between 400 and 470 nm (Aceto et al., 2014; Tamburini and Dyer, 2019). Moreover, the absorption characteristics vary depending on the dye preparation methods (Aceto et al., 2014; Gulmini et al., 2013). However, we observed some discrepancies in the curves obtained from the yellow reference samples in our study. The absorption characteristics of the yellow dyes in two *New Year* paintings were most similar to those of pagoda bud. However, this attribution cannot be confirmed using non-invasive techniques at present.

Furthermore, the visible reflectance spectra of the green pigment (a10) exhibited two maximum absorptions at 441 nm and 566 nm, similar to the superposition curves of a1 and a3 (Fig. 5c), suspecting a mixture of special pigments (a1) and yellow lakes (a3). The material costs can be reduced by mixing blue and yellow dyes rather than using green pigments, such as atacamite ($Cu_2(OH)_3Cl$) or malachite ($Cu_2(OH)_2CO_3$), to obtain a green hue.

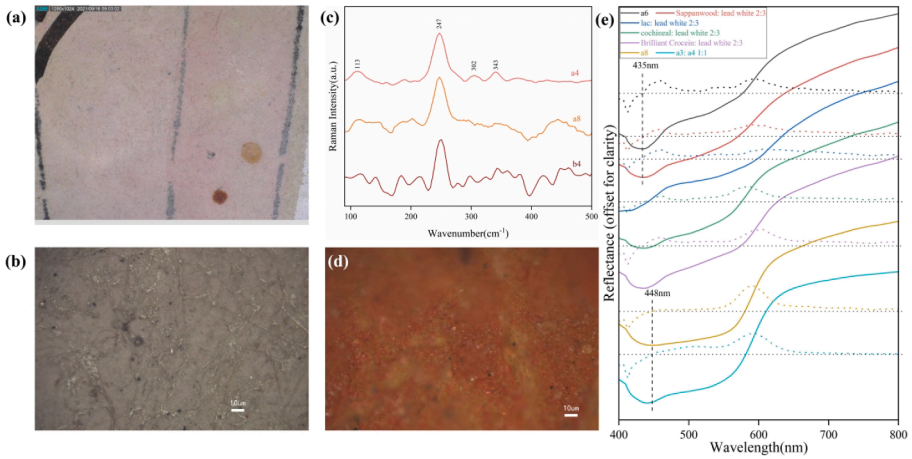

Fig. 6. Micrograph of areas of (a) a6; (b) a6; (d) a8. (c) Raman spectra obtained for a4, a8, and b4. (e) Reflectance spectra of a6, a8, sappanwood + lead white, lac + lead white, cochineal + lead white, Brilliant crocein + lead white, and a3 + a4. The dashed line of the same color is the first derivative of the reflectance spectrum.

3.3. Red, pink, and orange pigments

XRF images (Fig. 3a, Fig. 4a) showed a high abundance of Hg in both red robes (a4 and b4 in Fig. 1), indicating that the red pigment should be vermilion (HgS), which was also confirmed by Raman spectra with a strong band at 247 cm^{-1} assigned to vibration mode A1 for Hg-S as shown in Fig. 6c (Cosano et al., 2019). Vermilion was one of the most commonly used red pigments in ancient time and was widely used in many painted artworks (Li et al., 2020; Liu et al., 2013; Wang et al., 2021).

The pink pigment (a6) had a high abundance of Pb (Fig. 3a), most likely derived from lead white, while its Raman spectrum was not obtained due to the strong fluorescence. It was inferred after microscopic observation as shown in Fig. 6a and Fig. 6b that a6 should be a pink lake composed of a red dye and lead white. Four dyes were selected as reference dyes, including sappanwood (a plant dye most commonly found in folk paintings), lac, cochineal, and Brilliant Crocein (an early synthetic dye), and their reflectance spectra were compared with a6. The results (Fig. 6e) showed that reflectance spectra and the 1st derivative of both a6 and sappanwood had similar characteristics, with strong absorptions at 435 nm, indicating the pink lake may be a mixture of lead white and sappanwood, a kind of arbor, has been used for a long time in dyeing (Tamburini, 2019).

In addition, vermilion also was identified in the orange color using Raman spectroscopy (a8 in Fig. 6c). However, the micrograph (Fig. 6d) clearly showed the presence of a yellow dye made the orange color. Moreover, a8 and the mixture (a3 + a4) showed similar spectral features (Fig. 6e): their reflectance spectra generated characteristic maximum absorptions at around 448 nm, and the maximum peaks in their first derivative spectrum laid in the 595–600 nm range, which suggested that the orange pigment was made by mixing vermilion and a yellow dye, possibly pagoda bud mentioned above. Since the orange area was quite small, it may be easier and faster to mix the pigments that were already prepared and used for the *New Year* paintings to save the material costs.

3.4. Black, white, and gray pigments

The XRF results (Fig. 3a, Fig. 4a) showed that Pb was present in substantial amounts in the white areas of both paintings, suggesting lead white might be used. In addition, Pb was less abundance on the blue pants (a1) and the pink robe (a6) of *A Blessing from Bamboo*, suggesting that the pigments were probably mixed with lead white. The strong covering power of lead white makes it a popular candidate to mix with other pigments to obtain lighter shades of different colors. According to Joseph Needham (Needham et al., 1954), artificial lead white was available in China around 300 BCE. Lead white has been found on numerous painted artifacts in China from terracotta warriors and horses of the Qin Dynasty (Li, 1983) to many paintings of the Qing Dynasty. Moreover, lead white had also been identified in various oil paintings such as *Girl with a Pearl Earring* (Benquerenca et al., 2009; De Meyer et al., 2019), which proved that lead white was one of the most extensively used white pigments from antiquity to the early 20th century.

Raman spectroscopy (Fig. 7b) demonstrated the presence of carbon black in the regions a7, a9 and b8, where 1342 cm^{-1} was the D band in the lattice of carbon and 1568 cm^{-1} was attributed to the in-plane stretching vibration of carbon sp^2 hybridization (G band). A micrograph of the region a9 was shown in Fig. 7a. This gray tone was obtained by adding water to the ink to lighten the black color. Carbon black in

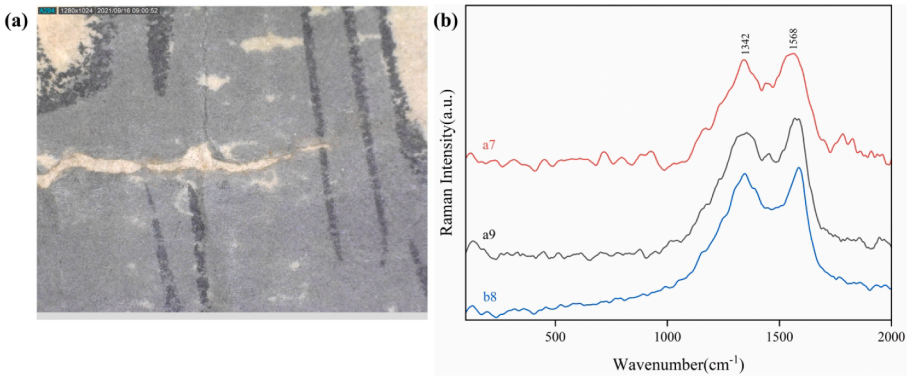

Fig. 7. (a) Micrograph of areas of a9. (b) Raman spectra obtained for a7, a9, and b8.

Table 1
List of pigments identified in the two *New Year* paintings considered in this study.

Paintings	Color	Detection points	XRF	Raman wavenumber (cm^{-1})	Pigment identified
A Blessing from Bamboo	blue	a1	Pb, K	848, 888, 960, 1074, 1169, 1259, 1302, 1372, 1471, 1591, 1654	a mixture of organic blue, organic purple, and lead white
	dark blue	a2	Fe, K	2151	Prussian blue
	yellow	a3	Pb, K, Ca	–	organic yellow
	red	a4	Hg	113, 247, 302, 343	vermilion
	white	a5	Pb	–	lead white
	pink	a6	Pb	–	a mixture of organic red and lead white
	black	a7	–	1342, 1568	carbon black
	orange	a8	Hg, Pb	113, 247	a mixture of a3 and a4 (vermilion)
	grey	a9	–	1340, 1568	carbon black
	green	a10	Ca	–	a mixture of a1 and a3
Attacking Mengzhou City	dark purple	b1	K	blue particle: 258, 559, 798, 1086, 1637; purple particle: 225, 415, 515, 644, 821, 908, 1163, 1290, 1369, 1521, 1585, 1617	a mixture of methyl/crystal violet and ultramarine blue
	light purple	b2	K	225, 415, 515, 644, 821, 908, 1163, 1290, 1369, 1521, 1585, 1617	methyl/crystal violet
	yellow	b3	–	–	organic yellow
	red	b4	Hg, Ca	113, 247, 343	vermilion
	bright yellow	b5		–	organic yellow
	blue	b6	Fe	2159	Prussian blue
	white	b7	Pb	–	lead white
	black	b8	–	1340, 1568	carbon black

New Year paintings was mainly derived from ink, which could be painted directly on the paper after adding glue. The earliest extant formula for making ink in China was recorded in the ancient Chinese agricultural book *Qi Min Yao Shu*. Pine-soot ink and oil-soot ink were two important artificial inks, mainly made from the soot of burning pine woods and oils, respectively. Since the oil-soot ink completely replaced pine-soot ink in the Ming and Qing dynasties, it is more likely that oil-soot ink was used in the *New Year* paintings (Ren, et al., 2018; Ren, et al., 2022).

4. Conclusion

In this study, we identified several natural dyes, pigments, and synthetic colorants used in Chinese *New Year* paintings through the application of non-invasive spectroscopic and imaging techniques (see Table 1). The use of a diverse range of dyes and pigments from various origins to create intricate and vibrant content in the *New Year* paintings demonstrates the exceptional painting skills of Yangliuqing craftsmen and their expertise and versatility in preparing coloring materials.

Traditionally, inorganic pigments and plant dyes from local sources were commonly used in Yangliuqing *New Year* paintings. However, with the emergence of Tianjin as a major trade center in the late 19th century, synthetic colorants manufactured in Europe began to appear in these paintings. Unlike traditional plant dyes and mineral pigments, which required the addition of gum and alum, synthetic colorants were easy to use and did not require the addition of other substances. As a result, they gradually replaced traditional paints due to their low cost and convenience. Our research not only sheds light on the trade of coloring materials between China and the West in the late 19th century but also reveals that the transition from traditional pigments to synthetic colorants was not immediate, as evidenced by the coexistence of both types of colorants in these two *New Year* paintings.

In summary, this study not only expands our understanding of the dyes and pigments used in woodblock *New Year* paintings, particularly during the late 19th and early 20th centuries when trade between China and the West was flourishing, but also provides crucial information for the preservation of these paintings and their colors.

Declaration of Competing Interest

The authors declare the following financial interests/personal relationships which may be considered as potential competing interests: Hui Zhang reports financial support was provided by National Social Science Fund. Hui Zhang reports financial support was provided by Fundamental Research Funds for the Central Universities.

Data availability

Data will be made available on request.

Acknowledgement

This study was financially supported by the Fundamental Research Funds for the Central Universities and National Social Science Fund (Grant Number: 19BKG45).

Appendix A. Supplementary material

Supplementary data to this article can be found online at https://doi.org/10.1016/j.jasrep.2023.104061.

References

Aceto, M., Agostino, A., Fenoglio, G., Idone, A., Gulmini, M., Picollo, M., Ricciardi, P., Delaney, J.K., 2014. Characterisation of colourants on illuminated manuscripts by portable fibre optic UV-visible-NIR reflectance spectrophotometry. Anal. Methods 6, 1488–1500. https://doi.org/10.1039/c3ay41904e.

Benquerenca, M.J., Mendes, N.F.C., Castellucci, E., Gaspar, V.M.F., Gil, F., 2009. Micro-Raman spectroscopy analysis of 16th century Portuguese Ferreirim Masters oil paintings. J. Raman Spectrosc. 40, 2135–2143. https://doi.org/10.1002/jrs.2383.

Bin, W., Hui, Y., Bovyn, G., Caen, J.M.A., 2017. Identification of pigments from "Zhenhai Temple", a Qing Dynasty export oil painting. Sci. Conserv. Archaeol. 29, 82–88 in Chinese.

Biron, C., Le Bourdon, G., Perez-Arantegui, J., Servant, L., Chapoulie, R., Daniel, F., 2018. Probing some organic ukiyo-e Japanese pigments and mixtures using non-invasive and mobile infrared spectroscopies. Anal. Bioanal. Chem. 410, 7043–7054. https://doi.org/10.1007/s00216-018-1305-2.

Biron, C., Mounier, A., Arantegui, J.P., Le Bourdon, G., Servant, L., Chapoulie, R., Roldan, C., Almazan, D., Diez-de-Pinos, N., Daniel, F., 2020a. Colours of the "images of the floating world". non-invasive analyses of Japanese ukiyo-e woodblock prints

(18th and 19th centuries) and new contributions to the insight of oriental materials. Microchem. J. 152, 104374 https://doi.org/10.1016/j.microc.2019.104374.
Biron, C., Mounier, A., Le Bourdon, G., Servant, L., Chapoulie, R., Daniel, F., 2020b. Revealing the colours of ukiyo-e prints by short wave infrared range hyperspectral imaging (SWIR). Microchem. J. 155, 104782 https://doi.org/10.1016/j.microc.2020.104782.
Caggiani, M.C., Acquafredda, P., Colomban, P., Mangone, A., 2014. The source of blue colour of archaeological glass and glazes: the Raman spectroscopy/SEM-EDS answers. J. Raman Spectrosc. 45, 1251–1259. https://doi.org/10.1002/jrs.4492.
Cavaleri, T., Giovagnoli, A., Nervo, M., 2013. Pigments and Mixtures Identification by Visible Reflectance Spectroscopy. Proced. Chem. 8, 45–54. https://doi.org/10.1016/j.proche.2013.03.007.
Cesaratto, A., Luo, Y.-B., Smith, H.D., Leona, M., 2018. A timeline for the introduction of synthetic dyestuffs in Japan during the late Edo and Meiji periods. Herit. Sci. 6, 22–33. https://doi.org/10.1186/s40494-018-0187-0.
Cesaratto, A., Leona, M., Pozzi, F., 2019. Recent Advances on the Analysis of Polychrome Works of Art: SERS of Synthetic Colorants and Their Mixtures With Natural Dyes. Front. Chem. 7, 105. https://doi.org/10.3389/fchem.2019.00105.
Confortin, D., Neevel, H., Brustolon, M., Franco, L., Kettelarij, A.J., Williams, R.M., Bommel, M.R.v.,, 2010. Crystal violet: Study of the photo-fading of an early synthetic dye in aqueous solution and on paper with HPLC-PDA, LC-MS and FORS. J. Phys.: Conf. Ser. 231, 012011 https://doi.org/10.1088/1742-6596/231/1/012011.
Cosano, D., Esquivel, D., Costa, C.M., Jimenez-Sanchidrian, C., Ruiz, J.R., 2019. Identification of pigments in the Annunciation sculptural group (Cordoba, Spain) by micro-Raman spectroscopy. Spectrochim. Acta A-Mol. Biomol. Spectrosc. 214, 139–145. https://doi.org/10.1016/j.saa.2019.02.019.
Cucci, C., Bracci, S., Casini, A., Innocenti, S., Picollo, M., Stefani, L., Rao, I.G., Scudieri, M., 2018. The illuminated manuscript Corale 43 and its attribution to Beato Angelico: Non-invasive analysis by FORS, XRF and hyperspectral imaging techniques. Microchem. J. 138, 45–57. https://doi.org/10.1016/j.microc.2017.12.021.
Daniel, F., Mounier, A., Pérez-Arantegui, J., Pardos, C., Prieto-Taboada, N., Fdez-Ortiz de Vallejuelo, S., Castro, K., 2016. Hyperspectral imaging applied to the analysis of Goya paintings in the Museum of Zaragoza (Spain). Microchem. J. 126, 113–120. https://doi.org/10.1016/j.microc.2015.11.044.
Daniel, F., Mounier, A., Pérez-Arantegui, J., Pardos, C., Prieto-Taboada, N., Fdez-Ortiz de Vallejuelo, S., Castro, K., 2017. Comparison between non-invasive methods used on paintings by Goya and his contemporaries: hyperspectral imaging vs. point-by-point spectroscopic analysis. Anal. Bioanal. Chem. 409, 4047–4056. https://doi.org/10.1007/s00216-017-0351-5.
De Meyer, S., Vanmeert, F., Vertongen, R., Van Loon, A., Gonzalez, V., Delaney, J., Dooley, K., Dik, J., Van der Snickt, G., Vandivere, A., Janssens, K., 2019. Macroscopic x-ray powder diffraction imaging reveals Vermeer's discriminating use of lead white pigments in Girl with a Pearl Earring. Sci. Adv. 5, eaax1975. https://doi.org/10.1126/sciadv.aax1975.
de Viguerie, L., Rochut, S., Alfeld, M., Walter, P., Astier, S., Gontero, V., Boulc'h, F., 2018. XRF and reflectance hyperspectral imaging on a 15th century illuminated manuscript: combining imaging and quantitative analysis to understand the artist's technique. Herit. Sci. 6, 11–23. https://doi.org/10.1186/s40494-018-0177-2.
de Viguerie, L., Pladevall, N.O., Lotz, H., Freni, V., Fauquet, N., Mestre, M., Walter, P., Verdaguer, M., 2020. Mapping pigments and binders in 15th century Gothic works of art using a combination of visible and near infrared hyperspectral imaging. Microchem. J. 155, 104674 https://doi.org/10.1016/j.microc.2020.104674.
dos Santos, H.C., Caliri, C., Pappalardo, L., Catalano, R., Orlando, A., Rizzo, F., Romano, F.P., 2018. Real-time MA-XRF imaging spectroscopy of the Virgin with the Child painted by Antonello de Saliba in 1497. Microchem. J. 140, 96–104. https://doi.org/10.1016/j.microc.2018.04.015.
Edwards, H.G.M., Benoy, T.J., 2007. The de Brecy Madonna and Child tondo painting: A raman spectroscopic analysis. Anal. Bioanal. Chem. 387, 837–846. https://doi.org/10.1007/s00216-006-0646-4.
Edwards, G., Villafana, T., 2020. Multi-analytic characterization of colorants in two impressions of an Utagawa Toyoharu perspective print. J. Cult. Herit. 45, 48–58. https://doi.org/10.1016/j.culher.2020.04.016.
Gulmini, M., Idone, A., Diana, E., Gastaldi, D., Vaudan, D., Aceto, M., 2013. Identification of dyestuffs in historical textiles: Strong and weak points of a non-invasive approach. Dyes Pigments 98, 136–145. https://doi.org/10.1016/j.dyepig.2013.02.010.
Hagan, E., Poulin, J., 2021. Statistics of the early synthetic dye industry. Herit. Sci. 9, 33–46. https://doi.org/10.1186/s40494-021-00493-5.
He, J., Zhao, F., Liu, J., Wu, Z., 2019. Study on the history of imported dyes in modern China: introducton of imported dyes. J. Silk 56, 109–114 in Chinese.
Kissell, L.N., Quady, T.K., Durastanti, D., Springer, S., Kenmotsu, J., Clare, T.L., 2022. A multi-analytical approach to identify red colorants on woodblock prints attributed to Suzuki Harunobu. Herit. Sci. 10, 94–113. https://doi.org/10.1186/s40494-022-00731-4.
Kogou, S., Lucian, A., Bellesia, S., Burgio, L., Bailey, K., Brooks, C., Liang, H.D., 2015. A holistic multimodal approach to the non-invasive analysis of watercolour paintings. Appl. Phys. A-Mater. Sci. Process. 121, 999–1014. https://doi.org/10.1007/s00339-015-9425-4.
Kokiasmenou, E., Caliri, C., Kantarelou, V., Germanos Karydas, A., Romano, F.P., Brecoulaki, H., 2020. Macroscopic XRF imaging in unravelling polychromy on Mycenaean wall-paintings from the Palace of Nestor at Pylos. J. Archaeol. Sci.: Reports 29, 102079. https://doi.org/10.1016/j.jasrep.2019.102079.
Leona, M., Decuzzi, P., Kubic, T.A., Gates, G., Lombardi, J.R., 2011. Nondestructive Identification of Natural and Synthetic Organic Colorants in Works of Art by Surface Enhanced Raman Scattering. Anal. Chem. 83, 3990–3993. https://doi.org/10.1021/ac2007015.
Li, Y.D., 1983. Painting pigments of Qin Terra cotta and history of pigments in Qin Dynasty. Archaeol. Cult. Relics 3, 62–65 in Chinese.
Li, Z.M., Wang, L.L., Chen, H.L., Ma, Q.L., 2020. Degradation of emerald green: scientific studies on multi-polychrome Vairocana Statue in Dazu Rock Carvings, Chongqing, China. Herit. Sci. 8, 64–75. https://doi.org/10.1186/s40494-020-00410-2.
Liu, Z., Han, Y., Han, L., Cheng, Y., Ma, Y., Fang, L., 2013. Micro-Raman analysis of the pigments on painted pottery figurines from two tombs of the Northern Wei Dynasty in Luoyang. Spectrochim. Acta A-Mol. Biomol. Spectrosc. 109, 42–46. https://doi.org/10.1016/j.saa.2013.02.015.
Liu, Z.F., Zhang, H., Zhou, W.H., Hao, S.C., Zhou, Z., Qi, X.K., Shi, J.L., 2019. Pigment identification on an undated Chinese painting by non-destructive analysis. Vib. Spectrosc. 101, 28–33. https://doi.org/10.1016/j.vibspec.2018.08.009.
Mazzinghi, A., Ruberto, C., Castelli, L., Czelusniak, C., Giuntini, L., Mando, P.A., Taccetti, F., 2021. MA-XRF for the Characterisation of the Painting Materials and Technique of the Entombment of Christ by Rogier van der Weyden. Appl. Sci. 11, 6151. https://doi.org/10.3390/app11136151.
Mounier, A., Denoel, C., Daniel, F., 2016. Material identification of three French medieval illuminations of the XVIth century by hyperspectral imaging (Treasury of Bordeaux Cathedral, France). Color Res. Appl. 41, 302–307. https://doi.org/10.1002/col.22042.
Mounier, A., Le Bourdon, G., Aupetit, C., Lazare, S., Biron, C., Pérez-Arantegui, J., Almazán, D., Aramendia, J., Prieto-Taboada, N., Fdez-Ortiz de Vallejuelo, S., Daniel, F., 2018. Red and blue colours on 18th–19th century Japanese woodblock prints: In situ analyses by spectrofluorimetry and complementary non-invasive spectroscopic methods. Microchem. J. 140, 129–141. https://doi.org/10.1016/j.microc.2018.04.023.
Needham, J., Yü, H.P., Djen, L.G., Ling, W., 1954. Science and Civilisation in China. at the Univ, Cambridge.
Oh, S., 2007. The Reinterpretation of Shaman Painting 'Sehwa' in Contemporary Korean Style Painting. J. Basic Des. Art 8, 435–451 in Korean.
Perez-Arantegui, J., Ruperez, D., Almazan, D., Diez-de-Pinos, N., 2018. Colours and pigments in late ukiyo-e art works: A preliminary non-invasive study of Japanese woodblock prints to interpret hyperspectral images using in-situ point-by-point diffuse reflectance spectroscopy. Microchem. J. 139, 94–109. https://doi.org/10.1016/j.microc.2018.02.015.
Pu, S.N., 2008. The history of Chinese New Year paintings art. Hunan Fine Arts Press, Changsha (in Chinese).
Pyong-Mo, C., 2006. Comparison between Korean Folk Paintings and Chinese Folk Nian Hua. Korean J. Folk Stud. 19, 183–217 in Korean.
Pyong-Mo, C., 2010. An Introduction to Vietnamese Folk Paintings. Suvannabhumi 2, 1–28 in Korean.
Ren, M., Wang, R.F., Yang, Y.M., 2018. Identification of the proto-inkstone by organic residue analysis: a case study from the Changle Cemetery in China. Herit. Sci. 6, 19–28. https://doi.org/10.1186/s40494-018-0184-3.
Ren, M., Guan, L., Wang, N., Xu, C.Q., Cui, Y.P., He, D.H., Wang, C.S., Yang, Y.M., 2022. Investigation of the manufacture development of early Chinese ink in the Western Han dynasty. Archaeom. 64, 1213–1225. https://doi.org/10.1111/arcm.12763.
Saverwyns, S., Currie, C., Lamas-Delgado, E., 2018. Macro X-ray fluorescence scanning (MA-XRF) as tool in the authentication of paintings. Microchem. J. 137, 139–147. https://doi.org/10.1016/j.microc.2017.10.008.
Sciutto, G., Frizzi, T., Catelli, E., Aresi, N., Prati, S., Alberti, R., Mazzeo, R., 2018. From macro to micro: An advanced macro X-ray fluorescence (MA-XRF) imaging approach for the study of painted surfaces. Microchem. J. 137, 277–284. https://doi.org/10.1016/j.microc.2017.11.003.
Seldes, A.M., Burucúa, J.E., Maier, M.S., Abad, G., Jáuregui, A., Siracusano, G., 1999. Blue Pigments in South American Painting (1610–1780). J. Am. Inst. Conserv. 38, 100–123. https://doi.org/10.1179/019713699806113484.
Stanley, T., 2015. Non-invasive Spectroscopic Investigation of a Sixteenth-Century Polychrome Aztec Picture Map on Deerskin. Restaur. 36, 183–210. https://doi.org/10.1515/res-2015-0001.
Tamburini, D., 2019. Investigating Asian colourants in Chinese textiles from Dunhuang (7th-10th century AD) by high performance liquid chromatography tandem mass spectrometry-Towards the creation of a mass spectra database. Dyes Pigments 163, 454–474. https://doi.org/10.1016/j.dyepig.2018.12.025.
Tamburini, D., Dyer, J., 2019. Fibre optic reflectance spectroscopy and multispectral imaging for the non-invasive investigation of Asian colourants in Chinese textiles from Dunhuang (7th-10th century AD). Dyes Pigments 162, 494–511. https://doi.org/10.1016/j.dyepig.2018.10.054.
Wan, L., Liu, Y., Dai, H.P., Feng, W., Zhang, J.W., 2019. Woodblock image decomposition of Chinese new year paintings. Multimed. Tools Appl. 78, 7621–7641. https://doi.org/10.1007/s11042-018-6447-x.
Wang, S.C., 2002. The history of Chinese New Year paintings. Beijing Industrial Art Press, Beijing (in Chinese).
Wang, S.C., 2005. The development history of Chinese New Year paintings. Tianjin People's Fine Arts Press, Tianjin (in Chinese).
Wang, X., Zhen, G., Hao, X.Y., Zhou, P., Wang, Z., Jia, J., Gao, Y., Dong, S.H., Tong, H., 2021. Micro-Raman, XRD and THM-Py-GC/MS analysis to characterize the materials used in the Eleven-Faced Guanyin of the Du Le Temple of the Liao Dynasty. China. Microchem. J. 171, 106828 https://doi.org/10.1016/j.microc.2021.106828.
Whitney, A.V., Van Duyne, R.P., Casadio, F., 2006. An innovative surface-enhanced Raman spectroscopy (SERS) method for the identification of six historical red lakes and dyestuffs. J. Raman Spectrosc. 37, 993–1002. https://doi.org/10.1002/jrs.1576.

Xiao, L., Wang, A., 2010. On the Continuity and Development of Mianzhu New Year Painting in Nowadays. Packag. Eng. 31, 132–135 in Chinese.
Zaffino, C., Passaretti, A., Poldi, G., Fratelli, M., Tibiletti, A., Bestetti, R., Saccani, I., Guglielmi, V., Bruni, S., 2017. A multi-technique approach to the chemical characterization of colored inks in contemporary art: The materials of Lucio Fontana. J. Cult. Herit. 23, 87–97. https://doi.org/10.1016/j.culher.2016.09.006.
Zhang, C., Huang, J.B., Zhu, T.Q., Zhang, R.L., 2021. Guangzhou Tongcao painting in late China Qing Dynasty (1840–1912 AD): technology revealed by analytical approaches. Herit. Sci. 9, 9–18. https://doi.org/10.1186/s40494-020-00472-2.

Identification of Fake Gold Gilding Material in the Ancient Wall Paintings by Mass Spectrometry Imaging

Sihan Zhao(1), Zhibo Zhou(2,3), Lin Zhang(4) and Hui Zhang(1,5)

(1) School of Art and Archaeology, Zhejiang University, Hangzhou 310028, China
(2) College of Cultural Heritage, Northwest University, Xi'an 710069, China
(3) Conservation and Restoration Department, The Kucha Academy of Xinjiang, Urumqi 830000, China
(4) Waters Corporation, Shanghai 201206, China
(5) Laboratory for Art and Archaeology Image of Ministry of Education, Zhejiang University, Hangzhou 310028, China

Keywords: fake gold, gilding material, tin leaves, wall paintings, DESI-MS

Tiny pieces of metallic foils (gold, silver or tin) were often used for decoration in ancient architecture, sculpture and paintings. Our previous study has shown that both tin and gold leaves were used as the gilding foils in Cave 171 of Kizil Grottoes (5th-7th Century A.D.), China [1]. Several gilding leaf samples from the wall paintings of Simsum Grottoes (China, 4th-8th Century A.D.) and Kizil Grottoes were determined as tin foil by scanning electron microscopy and energy-dispersive X-ray spectroscopy (SEM-EDS), but showed yellow color just as gold leaf, which is known as "fake gold", a phenomenon also appeared in medieval paintings in Europe [2,3]. To further investigate the fake gold gilding material, desorption electrospray ionization-mass spectrometry (DESI-MS) imaging method was applied on the both sides of tin leaf samples. Amur-cork tree (*Phellodendron amurense Rupr.*), a natural plant dye, was identified on the yellow tin leaves. This result was further confirmed by ultra-performance liquid chromatography-tandem mass spectrometry (UPLC-MS/MS) analysis. This is the first report about the exact composition of fake gold gilding material in ancient wall paintings along the Silk Road. The use of Amur-cork tree for fake gold is also quite different from the ancient Chinese archive such as *T'ien-kung k'ai-wu*, in which safflower oil was mentioned to be used as fake gold for silver gilding. Our results also demonstrate that DESI-MS imaging is capable of identifying and locating organic dyes on the surface of the artwork samples, which has great potential for the non-destrutive analysis of organic materials in precious heritage objects, addressing a number of questions of interest to artists, scientists, and conservators.

[1] A. Zhou Z, B. Ling S, C. Chen L, et al. Microchemical Journal 154, 2020, 104548.
[2] A. Mounier A, B. Daniel F, C. Bechtel F. Proceedings of the 37th International Symposium on Archaeometry, 2008, 273–278.
[3] A. Sandu I, B. MHD Sá, C. Pereira M C. Surface and Interface Analysis 43(8), 2011, 1134-1151.

课题参与证明

兹有浙江大学艺术与考古学院考古学专业博士生赵思涵同学（学号：12240009）于2020年9月至2023年8月参与由本人负责的国家社科基金一般项目“新疆克孜尔石窟壁画有机染料及其使用技法的研究”（项目编号：19BKG045），作为骨干成员在其中承担克孜尔石窟壁画中有机染料的质谱分析工作。

证明人：

2023年10月5日

浙江大学学科交叉预研专项项目

申报书

项目名称	丝绸之路沿线彩绘文物中有机染料的使用及其文化意义
涉及学科	考古学、药学
责任单位	艺术与考古学院
负 责 人	张晖 葛志伟
填表日期	2023.3

浙江大学社会科学研究院

2023 年 2 月制

<table>
<tr><td>项目名称</td><td colspan="6">丝绸之路沿线彩绘文物中有机染料的使用及其文化意义</td></tr>
<tr><td>涉及学科</td><td colspan="6">考古学、药学</td></tr>
<tr><td>负责人A</td><td>张晖</td><td>所属单位</td><td>艺术与考古学院、教育部哲学社会科学实验室-浙江大学艺术与考古图像数据实验室</td><td>职　　称</td><td colspan="2">教授</td></tr>
<tr><td>工号</td><td>0011030</td><td>所属学科</td><td>考古学</td><td>联系方式</td><td colspan="2">电话：13575764362
邮箱：huizhang@zju.edu.cn</td></tr>
<tr><td colspan="2">是否已受本年度基本科研业务费资助</td><td colspan="5">☑否　☐ 是，资助额度：_____万元</td></tr>
<tr><td>负责人B</td><td>葛志伟</td><td>所属单位</td><td>农生环学部</td><td>职　　称</td><td colspan="2">高级实验师</td></tr>
<tr><td>工号</td><td>0012461</td><td>所属学科</td><td>药学</td><td>联系电话</td><td colspan="2">13989462654</td></tr>
<tr><td colspan="2">是否已受本年度基本科研业务费资助</td><td colspan="5">☑ 否　☐ 是，资助额度：_____万元</td></tr>
<tr><td>预期成果形式</td><td>专著</td><td>论文</td><td>专利</td><td>报告</td><td colspan="2">其他：_____</td></tr>
<tr><td>预期成果数量</td><td>_____部</td><td>3 篇</td><td>_____项</td><td>_____篇</td><td colspan="2">_____项</td></tr>
<tr><td>项</td><td>姓名</td><td>性别</td><td>出生年月</td><td>所属单位</td><td colspan="2">研究专长</td></tr>
</table>

目组主要成员	赵思涵	女	1998.03	艺术与考古学院	文物保护
	陆诗燕	女	2000.3	农生环测试中心	质谱分析
	余亚清	女	1999.11	艺术与考古学院	光谱分析
	吕妙盈	女	2001.11	艺术与考古学院	物质文化研究
研究目的与意义	丝绸之路沿线分布着大量石窟寺，保存有许多精美的壁画、彩塑等，这一地区还出土了大量唐五代及以前的彩绘俑、纺织品和文书等，是丝绸之路兴衰的见证。其中颜料是这些彩绘文物的重要组成部分，它承载着文物的图像内容和色彩信息。长期以来，人们对古代壁画、彩塑等彩绘文物中使用颜料的认知大多以具有鲜艳色彩和较好稳定性的无机矿物颜料为主，而忽略了在彩绘文物中使用的有机染料。许多有机染料不仅价格昂贵，而且来源于特定的动植物，具有一定的地域特征，因此是当时彩绘制作工艺、不同地区之间文化交流和经济贸易等方面的重要实证。 不同于无机矿物颜料，有机材料特别容易发生降解，难以保存，例如变性、氧化、水解、交联等。因此，鉴别壁画、彩塑等彩绘文物中的有机染料具有很大的挑战性，不仅要处理复杂的混合物，包括各种可能存在的无机干扰物，同时染料、胶结材料以及其他材料之间可能会发生复杂的相互作用。考虑到彩绘文物的珍贵价值，通常仅有微量文物样品可用于实验分析，因此需要通过精确的分析检测技术对其成分和结构进行研究。文物分析中常用的光谱技术在染料鉴定中存在一定局限性，而液相色谱质谱联用技术（LC-MS）和解吸电喷雾电离质谱（DESI-MS）可以为壁画、彩塑等彩绘文物中的有机成分提供准确分析。本项目以新疆克孜尔石窟壁画、阿斯塔那墓葬彩塑、陕西墓葬壁画等丝绸之路沿线的彩绘文物为研究对象，采用液相色谱质谱联用技术和解吸电喷雾电离质谱为主要分析技术，研究这些彩绘文物中的有机染料种类及其制作工艺，并结合文献记载和考古发掘资料，进一步研究彩绘制作材料的传播路线，同时促进彩绘文物本体保护和工艺传承。 本项目将要研究的有机染料，大多来源于天然动植物，如靛蓝、黄檗、茜草、红花、紫胶等，并且是古往今来常见的药物成分。通过考古学与药学两个一级学科的交叉合作，利用药学学科的基础知识和先进技术手段，能够更加准确的分析和鉴别这些有机染料，助力丝绸之路沿线彩绘文物的研究。				